

Synthesis, Immobilization, MAS and HR-MAS NMR of a New Chelate Phosphine Linker System, and Catalysis by Rhodium Adducts Thereof

J. Guenther,^a J. Reibenspies,^a and J. Blümel^{a,*}

^a Texas A&M University, Department of Chemistry, P.O. Box 30012, College Station, TX 77842-3012, USA
Fax: (+1)-979-845-5629; phone: (+1)-979-845-7749; e-mail: bluemel@tamu.edu

Received: July 24, 2010; Revised: December 21, 2010; Published online: February 16, 2011

Abstract: A new class of tridentate phosphine ligands with the general formula $[\text{MeP}\{(\text{CH}_2)_x\text{PPh}_2\}_3]^+\text{I}^-$ ($x=4, 7, 11$) and $[\text{MeP}(\text{CH}_2\text{PPh}_2)_3]^+\text{OTf}^-$, has been synthesized and fully characterized. The linkers have been immobilized on silica with their phosphonium moieties *via* electrostatic interactions, and their mobility and leaching has been studied by solid-state HR-MAS (high-resolution magic angle spinning) NMR in various solvents. Immobilized Wilkinson-type rhodium complexes have been obtained by ligand exchange with the surface-bound linkers. The activities and lifetimes of the catalysts have been tested with respect to the

hydrogenation of 1-dodecene. The rhodium catalyst precursor bound by the immobilized linker $[\text{MeP}\{(\text{CH}_2)_7\text{PPh}_2\}_3]^+\text{I}^-$ led to material with the highest activity and lifetime, and it could be recycled for 30 times in a batchwise manner. The other catalysts show shorter lifetimes. For all catalysts the formation of rhodium nanoparticles with a narrow size distribution around 4 nm has been proven.

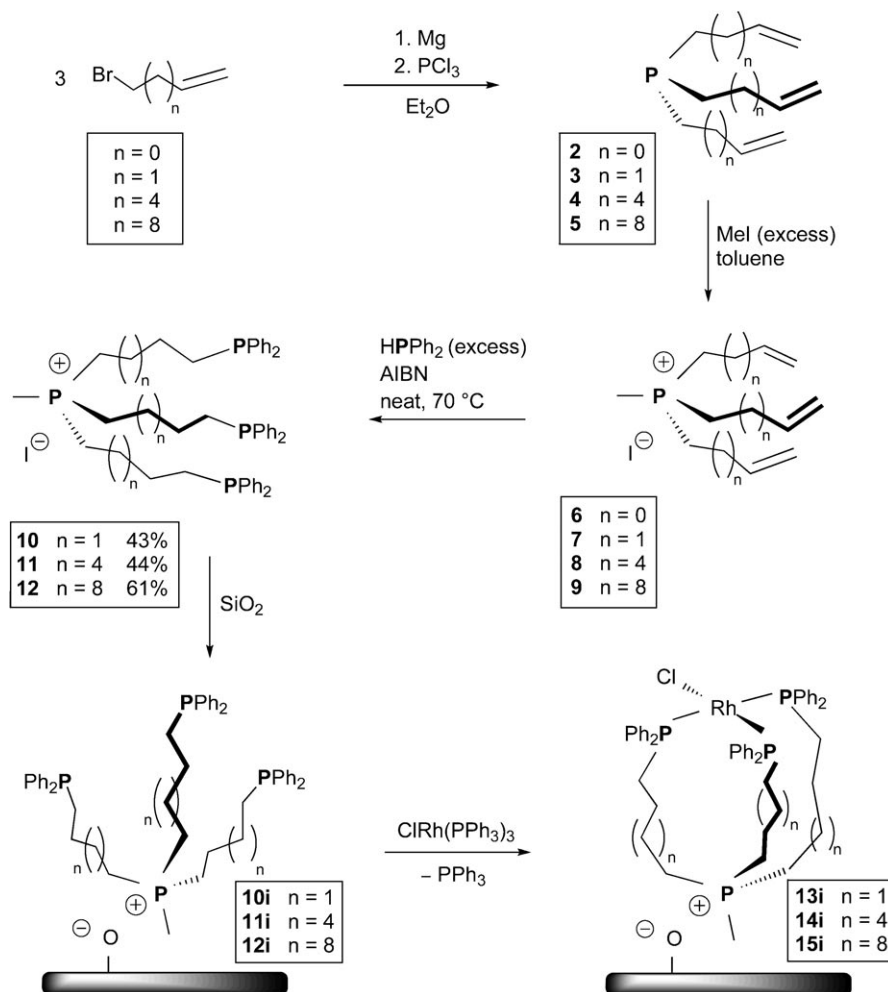
Keywords: chelate phosphines; immobilization; immobilized catalysts; phosphonium salts; rhodium complexes; rhodium nanoparticles

Introduction

Catalysts immobilized on solid supports are of growing academic and industrial interest, because they combine the advantages of homogeneous catalysts with those of heterogeneous catalysts. Immobilized catalysts are highly active and selective, while they can be easily separated from the reaction mixtures and recycled many times.^[1] The most favorable support material is silica,^[2] and bifunctional phosphines such as $\text{Ph}_2\text{P}(\text{CH}_2)_3\text{Si}(\text{OEt})_3$ or $\text{Ph}_2\text{P}(\text{CH}_2)_3\text{PPh}(\text{CH}_2)_3\text{Si}(\text{OEt})_3$ are popular linkers.^[3,4] They have led to very successful immobilized nickel^[3] and rhodium^[4] catalysts for cyclotrimerizations of acetylenes and olefin hydrogenations. To further improve this type of immobilized catalysts, two remaining problems have to be solved. (i) The catalysts, especially in their activated form, can decompose if they come into contact with the reactive oxide surface. This is, for example, obvious in the gradually darkening grey color of the originally white, bright yellow, or red catalysts with every recycling step. At the moment, this problem might only be ameliorated by the additional step of “end-capping” of the oxide surface with SiMe_3 groups after the immobilization of the catalyst,^[2] a procedure that many catalysts cannot tolerate. (ii) For the previ-

ously studied nickel^[3] and rhodium^[4] catalysts, which have been obtained by ligand exchange with $\text{CIRh}(\text{PPh}_3)_3$ (**1**), we could prove that dimerization or agglomeration of the surface-bound catalysts leads to their deactivation^[4] or loss of selectivity.^[3] The dimerization can be prevented by diluting the catalysts on the surface.^[4] However, this is less desirable in an industrial setting, because it increases the amount of bulk material per metal center, leading to bigger, more expensive reactors with correspondingly larger amounts of solvents and ensuing safety issues.

Linkers play a crucial role for all immobilized catalysts.^[1d] Therefore, problems (i) and (ii) can be solved by new generations of linkers. One successful approach we explored recently makes use of rigid tetraphenyl-element scaffolds based on the tetrahedral $[\text{R}_2\text{P}(p\text{-C}_6\text{H}_4)]_4\text{E}$ ($\text{E}=\text{C}, \text{Si}, \text{Sn}$; $\text{R}=\text{alkyl}, \text{aryl}$) structural units.^[5] However, chelate versions of these rigid linkers for better coordination and retention of the metal centers have not yet been synthesized. An alternative for solving both problems (i) and (ii) would be to use long alkyl chains, draped around the metal center in a chelating arrangement, to protect the catalytically active metal centers. Even one alkyl chain has some protecting effect. For example, recently we found that a Pt complex containing a long alkyl chain



Scheme 1. Syntheses of the monodentate phosphines **2**–**5**, their phosphonium salts **6**–**9**, and the chelate ligands **10**–**12**, their immobilized versions **10i**–**12i**, and the surface-bound Rh complexes **13i**–**15i**.

does not decompose on silica,^[6] although analogous Pt complexes with triaryl ligands do. Three chelating alkyl chains should protect a metal center optimally.

Regarding their design, these alkyl linkers should be robust, and not decompose on the surface, as bisphosphinoamines^[7a] or dppm-type linkers,^[7b] for example, do. The ethoxysilane linker EtOSi(CH₂PPh₂)₃ with the shortest possible alkyl chains is not sensitive in solution, but it obviously has too short a distance between the phosphine and the reactive ethoxysilane groups and decomposes on a silica surface, while EtOSi[(CH₂)₂PPh₂]₃ survives.^[8] Alkyl chains with 7 or 11 methylene groups between the phosphine and ethoxysilane groups, however, led to mono- and bidentate linkers with reduced oxygen sensitivity, that can cleanly be immobilized on oxide supports.^[9]

Furthermore, results with Wilkinson-type catalysts tethered to the support by linkers with long alkyl chains show that they display higher activity and better recycling characteristics than catalysts bound by shorter linkers,^[4] even when the latter are chelating

and the former only monodentate. This might be due to the fact that longer alkyl chains allow increased mobility of the immobilized catalyst and thus help to mimic homogeneous catalysis. One more positive effect of longer chains is that not only conventional solid-state CP/MAS (cross-polarization with magic angle spinning) or MAS NMR^[10] can be measured, but the HR-MAS (high-resolution magic angle spinning) signals of species with alkyl chains that are sufficiently mobilized in the presence of a solvent are extremely narrow.^[7a,8,9,11]

Here, we present a new class of chelating tridentate phosphine ligands with long alkyl chains that are immobilized *via* electrostatic interactions of phosphonium moieties with a silica surface. They are characterized by solid-state NMR, and their leaching has been studied. The long alkyl chains increase the mobility of the bound Wilkinson-type catalysts and in this way optimally mimic a homogeneous scenario for the respective catalysts. The three alkyl chains per metal center are also expected to prevent dimerization of the bound

complexes, because, when arranged in a balloon-type manner, they cannot interpenetrate the alkyl chains of a neighboring molecule. Furthermore, since the “balloon” cannot roll over, any deactivation by contact with the reactive support surface should be impossible. The catalytic activities, selectivities, and lifetimes are studied with respect to olefin hydrogenation.

Results and Discussion

Synthesis of the Phosphine Linkers

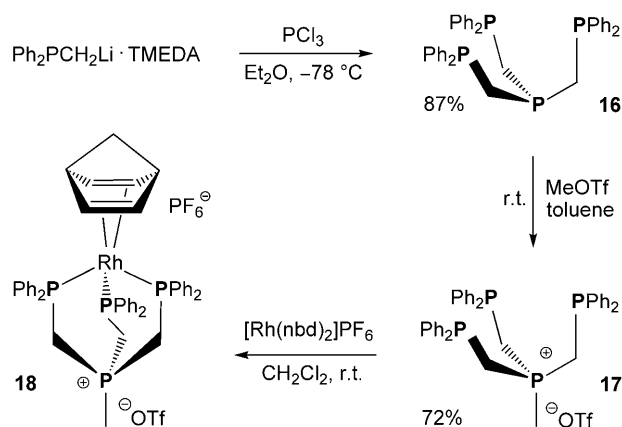
The phosphine ligand **3** has been synthesized starting from the corresponding commercially available bromo compound $\text{Br}(\text{CH}_2)_2\text{CH}=\text{CH}_2$, according to the procedure by Clark and Hartwell^[12a] (Scheme 1). The ^1H ,^[12a,b] ^{31}P ,^[12a] and ^{13}C ^[12c] NMR data are in accordance with the literature values. It should be noted that we were not able to isolate the phosphine $\text{P}(\text{CH}_2\text{CH}=\text{CH}_2)_3$ (**2**) in high yields in an analogous manner, most probably because the allyl substituents are vulnerable to polymerization or formation of five-membered rings *via* radicals.^[13] The phosphines **4** and **5** have been synthesized from the corresponding bromoalkenes as described by the Gladysz group.^[14] Ligand **16** (Scheme 2) with the shortest possible alkyl chain could be obtained in a very good yield of 87% by reacting $\text{Ph}_2\text{PCH}_2\text{Li}\cdot\text{TMEDA}$ ^[15] with PCl_3 . The data of **16** are in accordance with the data obtained for **16** synthesized from $\text{P}(\text{CH}_2\text{SiMe}_3)_3$ and ClPPh_2 .^[16] The phosphonium salts **7–9** (Scheme 1) have been synthesized in quantitative yields by stirring the corresponding phosphines **3–5** with an excess of CH_3I in toluene overnight. The methyl phosphonium salt $[\text{CH}_3\text{P}(\text{CH}_2\text{CH}=\text{CH}_2)_3]^+\text{I}^-$ (**6**) has been obtained by the one-pot reaction described in the Experimental Section, but during the subsequent hydrophosphination with AIBN again polymerization or a ring forma-

tion *via* radicals^[13] takes place, and therefore we have not pursued the linker with C_3 chains any further.

Methyl iodide as the quaternizing reagent for **16** led to a mixture of different phosphonium salts. Therefore, methyl triflate has been applied as a more selective quaternizing agent that alkylated only the most basic, the trialkylphosphine moiety of **16** (Scheme 2). The purification process was also facilitated by this reagent, and therefore clean **17** has been obtained in a good overall yield of 72%. Crystals suitable for X-ray structure determination^[17] (Figure 1) could be grown from an acetonitrile solution. As with the X-ray structure of the analogous compound $\text{EtOSi}(\text{CH}_2\text{PPh}_2)_3$ ^[8] the orientation of the phosphine groups is not preorganized for coordination, but dominated by the crystal packing. As expected, the triflate counteranion occupies the sterically least crowded space close to the methyl group of the phosphonium moiety. This constellation indicates that the linker **17** would indeed “stand upright” on the surface, when the phosphonium group is bound to the silica *via* electrostatic interactions (see below).

The triphosphines **10–12** (Scheme 1) have been obtained from **7–9** by applying an excess of HPPH_2 and, with respect to the whole molecule, a stoichiometric amount of AIBN as the radical source, slightly modifying the procedure described by Stelzer.^[18] Photochemical hydrophosphination without a radical forming reagent, as successfully applied previously,^[9,19] is possible here, but the reaction is more sluggish in the final stage. Overall, the general synthesis route for this ligand class, as outlined for specific cases in Scheme 1, is very versatile, as the chain lengths, the substituents at phosphorus, and the counteranions can be varied easily.

The presence of the phosphonium functionality does not disturb the coordination of the phosphine groups to metal centers. This has been demonstrated



Scheme 2. Syntheses of ligand **16**, its phosphonium salt **17**, and the Rh complex **18**.

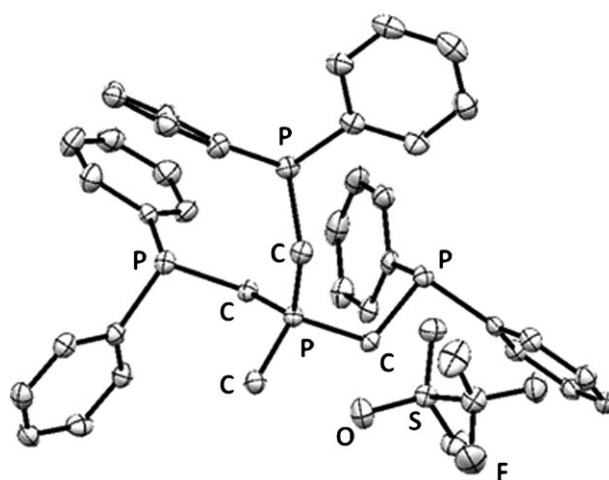


Figure 1. Single crystal X-ray structure of chelate ligand **17**.^[17]

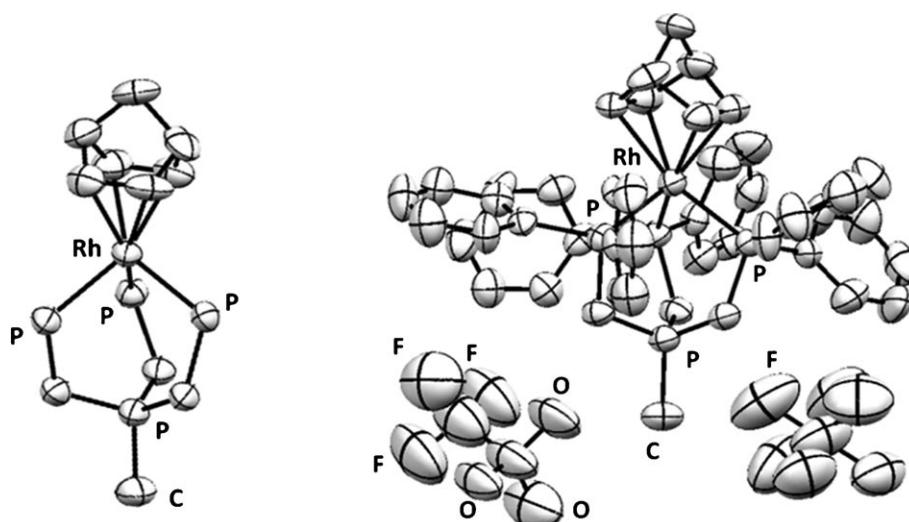


Figure 2. Single crystal X-ray structure of the Rh norbornadiene complex **18**.^[20] In the left presentation the counteranions OTf^- and PF_6^- , and the phenyl rings have been removed for clarity.

by the synthesis of **18** by reacting **17** with the norbornadiene complex $[\text{Rh}(\text{nbd})_2]\text{PF}_6$. The Rh complex has been fully characterized, and a single crystal X-ray structure^[20] has been obtained (Figure 2). The cation incorporating the Rh center is well defined, and overall the structure of **18** resembles the analogous Si-triphos^[21a] and triphos^[21b] Rh structures. The coordination of all three phosphine groups of **16** is obvious, as it is the case in an analogous methoxy-norbornadienyl Rh complex,^[22] as well as, for example, in various other tripod Rh^[23a] and Cu^[23b] complexes, and Sn,^[23c] Ir,^[23d] and Rh^[23e] complexes with borate tripod ligands. In contrast to these systems, **18** needs two counteranions to satisfy the positive charges of the Rh(I) center and the phosphonium ligand. Although the counteranions are less well defined, it is obvious from the structure that OTf^- and PF_6^- each have their specific place in the lattice and are not interchangeable. Interestingly, the closest counteranions in the lattice are both located at the same side of the complex, a fact that should facilitate the later well-defined binding of **18** to the silica surface. Furthermore, the phenyl rings are fanning out of the ligand, and thus might form a protecting “umbrella” that prevents the interaction of the Rh center with the reactive surface.

Immobilization of the Phosphine Linkers and Rh Complexes

One conventional way of binding metal complexes to oxide surfaces is, for example, using ethoxysilane containing linkers,^[2–4,7–9,11,24] such as $(\text{EtO})_3\text{Si}(\text{CH}_2)_3\text{PPh}_2$,^[24a] which form covalent Si–O–Si bonds with silica. Under certain conditions, however, the

ethoxysilane linkers can leach from the surface,^[24a] and furthermore the ethoxysilanes can lead to the *in situ* quaternization of the phosphine groups.^[25] We have applied this reaction recently to bind rigid tetraphenyl-element phosphine linkers without intramolecular ethoxysilane groups to silica supports.^[5] In the course of these studies we found that phosphonium salts are also bound strongly *via* electrostatic interactions to the oxide support,^[5,25] and that preformed phosphonium salts can be immobilized directly on oxide supports, without addition of alkoxy silanes.^[25] Therefore, besides their applications as flame retardants and polymerization starters, their interesting NMR characteristics,^[5,25,26] and previous applications for ionic liquids^[27] and liquid-liquid biphasic catalysis,^[28] as fluoride ion sensors^[29a] and chelators,^[29b] and as dihydrogen cleavage reagents,^[30] we can use phosphonium salts also as linkers now, which tether a catalyst to an oxide support.

The linkers **10–12** have been immobilized on silica to give **10i–12i** according to the straightforward standard procedure of stirring the mixture in toluene overnight at 50 °C. The counteranion does not play a crucial role for the immobilization of phosphonium salts on silica, and therefore **17i** with the triflate instead of the iodide counteranion could be generated by the same procedure. The resulting surface coverages are given in Table 1, together with the data for the corresponding immobilized Rh complexes, which have been obtained by ligand exchange at room temperature (**13i–15i**, Scheme 1), and reaction of **18** with silica to give **18i**. Although this work focuses on silica as the support, it should be mentioned that other oxide supports like alumina are favorable for phosphonium immobilization, too. The experimental maximal surface coverages for a monolayer of linker or

Table 1. Surface coverages^[a] of the modified silica **10i–15i** and **17i–21i** with the corresponding molecular species **X** (**10–15**, **17–21**).

Material	Molecules per 100 nm ² SiO ₂	mg of X per g SiO ₂	mmol of X per g SiO ₂
10i	3.25	36	0.041
11i	2.14	28	0.027
12i	1.57	24	0.020
17i	2.88	28	0.036
13i	3.25	42	0.041
14i	2.14	31	0.027
15i	1.57	27	0.020
18i	2.88	36	0.036
19i	34.3	147	0.427
20i	47.7	304	0.593
21i	39.3	238	0.489

^[a] All surface coverages correspond to 25% of the maximal coverage of the surface with a monolayer of the molecular species **X**, with the exception of **19i–21i**, where the surface coverage is 100%.

Rh complex on the silica surface have always been below the theoretically possible surface coverage. A rough estimate of the calculated maximal surface coverage can be obtained by using the linker chain length, including the phenyl groups, as the radius of a circle that would describe the footprint of the molecule if it was planar. For example, the chain lengths for **10** and **11** can be estimated to be 11.3 and 14.9 Å, respectively, and their (flat) foot print would be about 401 and 698 Å². Taking into account that only 78.5% of a flat surface can be filled with circles, this would translate into surface coverages of about 20 molecules per 100 nm² surface for **10i** and about 11 per 100 nm² for **11i**. The experimentally determined maximal surface coverages of about 14 and 8 molecules of **10i** and **11i** on 100 nm² of silica surface are lower, most probably due to the fact that favorable binding sites are not homogeneously distributed on the surface. Additionally, the narrow ends of the irregular pores, which count for the silica surface area when determined by BET measurements, might not be accessible for the rather large linker systems **10i–12i**. The surface coverages with the model phosphonium salts **19–21** are much higher (Table 1 gives the maximal experimental coverages), because the chains are shorter without the extending diphenylphosphine groups, and this leads to smaller foot prints. Most importantly, while statistically many linkers are still in contact with each other on the surface, when they are immobilized with maximal coverage, at 25% of the maximal loading the linkers are well separated from each other. This means that the Rh complexes immobilized with 25% of the maximal coverage should not be able to dimerize and therewith lose their catalytic activity prematurely.

The most powerful method for characterizing all surface-bound species is solid-state NMR spectroscopy.^[10] For the chemistry presented here, ³¹P is the analytically most valuable nucleus. Whenever the materials or molecules are rigid by nature, the classical way of measurement, which involves filling the dry material into a rotor and spinning with the magic angle (MAS) while cross-polarizing (CP) the proton magnetization, is the only option.^[5a] Possible drawbacks of CP/MAS are that the signals can no longer be integrated, and that at higher rotational frequencies the Hartmann–Hahn matching pattern splits into separate bands and signal intensity might be lost.^[10d]

However, in cases where the species possess some degree of motional freedom in the presence of a solvent, spinning a slurry of the material reduces the line widths substantially in an HR-MAS (high-resolution MAS)^[11] spectrum. Problems associated with CP are avoided, because HR-MAS spectra are best recorded with high-power decoupling only.^[11a] Our surface-bound linkers **17i** and **10i–12i** with their long flexible alkyl chains are sufficiently mobile in the presence of a solvent such as benzene to be amenable to HR-MAS. Figure 3 shows for **11i** as an example that due to the mobilizing effect of the solvent, combined with MAS, very narrow lines can be obtained with HR-MAS. The half-widths of the HR-MAS signals (*middle*) for both the phosphonium and phosphine moiety of **11i** are, with 92 and 73 Hz, nearly as small as those in the solution spectrum (*bottom*). In contrast to this, the corresponding signals of the classical MAS spectra of the dry material **11i** are much broader with 421 and 635 Hz. All chemical shifts and half-widths of the ³¹P MAS signals of the dry materials **10i–12i** and **17i**, and for their HR-MAS resonances are given in Table 2. As expected, the longer the alkyl chains, the higher is the mobility in the presence of the solvent, in accordance with the results of a study with monodentate, covalently bound linkers with long alkyl chains.^[9] But even for the linker **17i** with the shortest possible alkyl chain, the HR-MAS signals show sub-

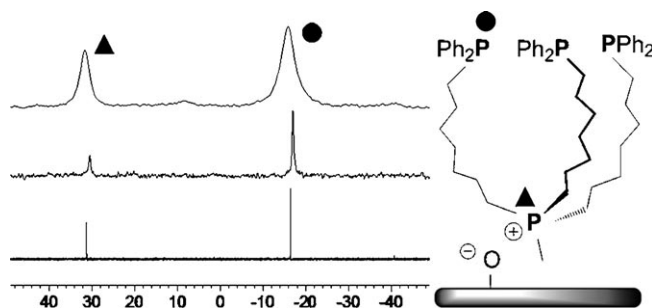


Figure 3. ³¹P NMR of **11i** (solution in C₆D₆, *bottom*), ³¹P HR-MAS of a slurry of **11i** with C₆D₆ (*middle*, spinning frequency 2 kHz), and ³¹P MAS NMR of dry **11i** (*top*, rotational frequency 4 kHz).

Table 2. ^{31}P MAS and HR-MAS NMR chemical shifts δ and signal half-widths $\nu_{1/2}$ for the phosphonium and phosphine signals (P⁺/P) of the linker-modified silica **10i–12i** and **17i** with maximal surface coverages (values for 25% coverage see Table 1). Rotational frequencies were 4 kHz for MAS measurements of dry materials, and 2 kHz for HR-MAS of slurries with C_6D_6 .

Material (P ⁺ /P)	$\delta(^{31}\text{P})$ (MAS) [ppm]	$\delta(^{31}\text{P})$ (HR-MAS) [ppm]	$\nu_{1/2}$ (MAS) [Hz]	$\nu_{1/2}$ (HR-MAS) [Hz]
17i	35.0/–29.2	33.7/–31.2	835/1780	300/505
10i	31.8/–15.9	30.0/–17.8	666/1448	604/239
11i	31.5/–15.9	30.4/–17.0	421/635	92/73
12i	31.6/–16.0	30.4/–16.9	352/416	100/39

stantially narrower lines, in accordance with the case of a covalently bound tripod-type ethoxysilane containing linker.^[8] When the surface coverage with linker is lowered to 25% of the maximal coverage, typically the signal half-widths increase. For example, the half-width for the phosphonium (phosphine) moiety of **11i** increases from 92 (73) to 278 (189) Hz. This again corroborates former results that have been obtained without spinning.^[24a] The lower surface coverage leads to reduced mobility of the phosphine group, because now there are enough surface sites left for the phosphine to adsorb. This in turn also reduces the rotational and overall mobility of the phosphonium group.

Interestingly, although the effect is not as pronounced as with the phosphine groups, even for the phosphonium ^{31}P HR-MAS signals of all surface-bound linkers the line-widths become smaller (Table 2). This indicates that in spite of the strong electrostatic interactions with the surface some mobility of the phosphonium moiety must be possible. Preliminary studies using the deuterated phosphonium salt $[\text{Ph}_3\text{PCD}_3]\text{I}$ bound to the silica surface *via* electrostatic interactions prove that there is no translational motion of the salt on the surface in the absence of a solvent. Whether the mobility of the linkers presented here is of a wagging or rotational type, will be the subject of a future, more detailed study. Most important with respect to catalysis is that the phosphine groups, and therewith the linker chains, are sufficiently mobile in a solvent to allow the later bending towards and coordination of the Rh complex. Furthermore, since translational mobility of the linkers can be excluded, the catalysts **13i–15i** should not be vulnerable to deactivation by dimerization.^[4]

One key question in our quest for the optimal immobilized catalyst is whether the catalytic activity and selectivity depend on the chain length and therewith the mobility of the linker and the catalyst. The more mobile the immobilized catalyst, the better it should

be able to simulate the performance of a homogeneous catalyst. As it is already known from earlier studies without sample rotation,^[24a] the ^{31}P NMR line-widths obtained from slurries of immobilized linkers are dependent on the solvent. In general, the less viscous and more polar the solvent is, the narrower are the signals. This is in accordance with the ^{31}P HR-MAS signals of the linkers presented here, so even with spinning at 2 kHz the solvent plays a major role for the spectrum quality. As an example, **12i** has also been measured in the presence of a variety of organic solvents other than benzene, and the resulting phosphine signals are displayed in Figure 4. The chemical shifts change over a range of maximally 0.4 ppm in the different solvents, which does not exceed the chemical shift changes one would find in solution. The line-widths are smallest with 20–24 Hz for the least viscous and most polar solvents, such as dichloromethane, acetonitrile and methanol, while the unpolar hexane leads to a comparatively broad line with a half-width of 134 Hz. However, while the linkers **10i–12i** and **17i** are rather robust, taking the coordinated metal complexes into account, non-protic and non-coordinating solvents are preferred for catalysis. Fortunately, the line-widths of **12i** in toluene (26 Hz) and benzene (43 Hz) imply that the linkers are still very mobile under the conditions of catalysis (Figure 4, Table 2). Therefore, toluene as the solvent for the Rh catalysts **13i–15i** and **18i** should provide conditions as close as possible to homogeneous catalysis with respect to catalyst mobility.

The linkers **10i–12i** and **17i** are bound to the support *via* electrostatic interactions of the phosphonium groups with the silica surface. While covalently bound linkers such as ethoxysilanes show some detachment from the surface under harsh conditions,^[24a] for surface-bound phosphonium salts the database is rather slim. Our preliminary experiments show that the

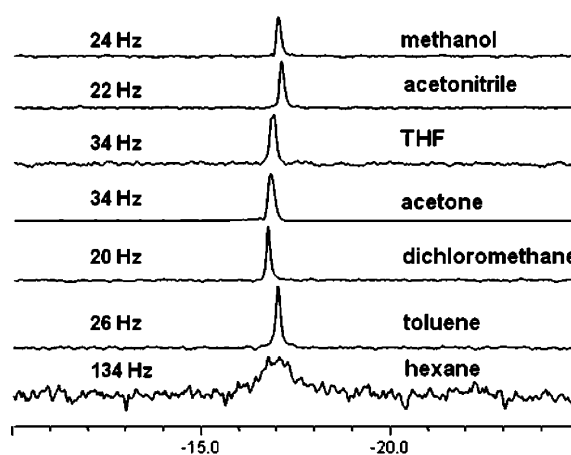


Figure 4. ^{31}P HR-MAS lineshapes with indicated half-widths (left), and signal positions for **12i** in the corresponding solvents. Rotational frequency 2 kHz.

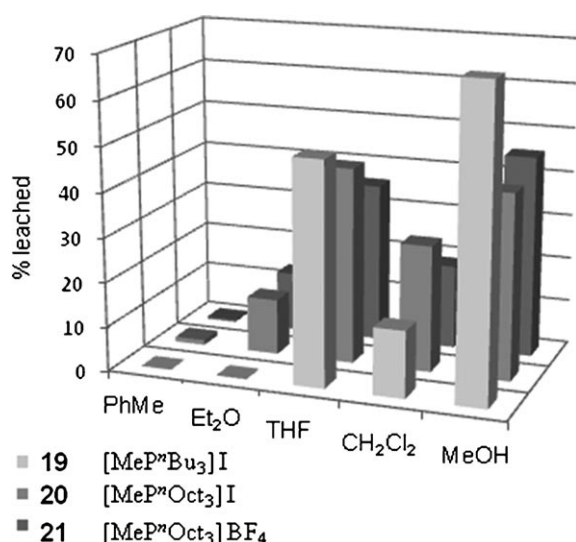


Figure 5. Graphic display of the leaching studies for the model phosphonium salts **19–21**. Leaching test: 400 mg of functionalized SiO₂ were suspended in the respective solvent and stirred for 24 h at room temperature. The amount of leached phosphonium salt in the supernatant was determined gravimetrically.

binding of tetraarylphosphonium salts to a silica surface is rather strong, and arylphosphonium salts proved impossible to remove from the support in substantial amounts by ion exchange or other reagents without dissolving the oxide support.^[5a] However, the solubility of the molecular phosphonium salts in the given solvents might play a role, and it should be higher for alkylphosphonium salts. Naturally, leaching due to linker detachment is a major issue for immobilized catalysts, and therefore we probed the leaching of alkylphosphonium salts quantitatively and in detail. In order to be able to work with large quantities and determine the leaching gravimetrically, while avoiding the expensive bromoalkene starting materials, we synthesized the phosphonium salts **19–21** (Figure 5) as model compounds and immobilized them with maximal surface coverage as **19i–21i** (Table 1). The leaching test revealed that practically no leaching occurs in non-polar solvents. Most importantly, the solvent used for the catalysis, toluene, does not detach measurable amounts of the phosphonium salts from the surface (Figure 5). However, polar and protic solvents, such as THF and methanol should be avoided as reaction medium for catalysis, since they lead to major detachment of the linker system from the SiO₂ surface. Hereby, the phosphonium salt with the shortest alkyl chains, **19i**, is most vulnerable to leaching. Interestingly, the binding is practically independent of the nature of the counteranion. This indicates that, for the tested salts, the electrostatic interactions are not substantially augmented by additional F...H hydrogen bonds between the F atoms of the BF₄⁻ counteranion and pro-

tons of the surface silanol groups,^[31] or the formation of new boron-containing species on the surface.^[32] Rather, the solubility of the phosphonium salts in the corresponding solvents and the ability of the solvent to replace the salts from the surface seem to play major roles. This is reflected in the fact that THF and methanol lead to the largest amounts of detached phosphonium salts from the surface. Toluene is the most favorable solvent for later catalysis, as it hardly leads to any leaching (Figure 5). As compared to the surface-bound model phosphonium salts **19i–21i**, the linkers **10i–12i** and **17i** should be somewhat more robust towards leaching, or else one would have detected the signals of free phosphines in solution in the HR-MAS spectra of Figure 4. Probably, the diphenylphosphine groups reduce the solubility and additionally function as a shield against detachment by the solvents. The single-crystal X-ray structure of **18** with its “umbrella” of phenyl groups (Figure 2) supports this assumption.

Immobilized Rhodium Catalysts

The immobilized Rh complexes **13i–15i** have been obtained from **10i–12i** by ligand exchange with Wilkinson's catalyst ClRh(PPh₃)₃ (**1**) at room temperature (Scheme 1). With 25% surface coverage of the linkers only one Rh center should be bound per immobilized linker molecule. The immobilized complex **18i** has been obtained by directly attaching **18** (Scheme 2) on the silica surface. The catalyst obtained after immobilizing **17** to give **17i**, and then treating it with **1** displayed catalysis characteristics identical with those of **18i**. The ³¹P MAS spectra prove that, after washing the materials thoroughly, there is no adsorbed PPh₃ left. Furthermore, no uncoordinated linker phosphines are present, and most importantly, no phosphine oxide signals with their characteristic chemical shift anisotropy (CSA) pattern.^[10a,25] This is, for example, shown in the spectrum of **15i** in Figure 6 (bottom). The phosphonium signal and the signal of the phosphines in *trans* positions to each other over-

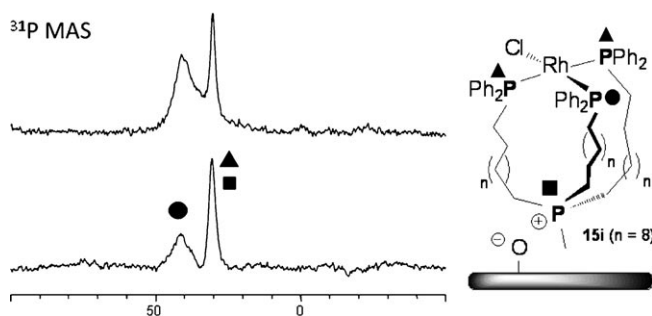
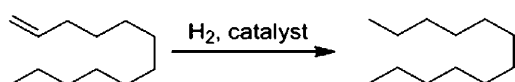


Figure 6. ³¹P MAS spectra of catalyst **15i** before (bottom) and after (top) catalysis.

lap at about 30 ppm, while the resonance of the phosphorus nucleus *trans* to Cl appears at about 41 ppm. Overall the ^{31}P MAS spectrum resembles the ones of various immobilized Wilkinson-type Rh complexes that we studied earlier.^[4] We could prove that in toluene, as anticipated from the linker leaching studies described above, all catalysts are firmly tethered to the support and that no noticeable leaching of the ligand or the metal center into solution occurs, even after stirring the material for a prolonged period of time in toluene.

Olefin hydrogenation is one of the best developed and most important catalytic reactions in academia and industry,^[33] therefore we use the catalytic hydrogenation of 1-dodecene as a model test reaction (Scheme 3). This also allows the comparison with earlier results of our group^[4] and others,^[34] especially since we retain the standard reaction conditions (Scheme 3). The only difference here is that the catalysts bound by the new alkylphosphine ligands need a slightly higher temperature of 60 °C to perform within reasonable time frames. As expected from our earlier work on hydrogenation catalysis,^[4a,b] reducing the surface coverage with catalyst to 25% of the maximal coverage prevents the dimerization of the Rh catalysts, and leads to increased catalytic activity. These early results also corroborated the assumption that the linkers and thus metal centers are initially evenly distributed on the surface, and do not form patches or clusters. The results presented here are in accord with this assumption. For example, when **15i** with maximal surface coverage (100%, 6.28 molecules per 100 nm² SiO₂ surface, 108 mg of **15** per g of SiO₂, 0.08 mmol of **15** per g of SiO₂) is used for catalysis, only about 50% H₂ conversion is obtained after 20 h of reaction time. With 25% surface coverage (data in Table 1), quantitative hydrogenation of 1-dodecene is achieved within 10 h. Therefore, if not mentioned otherwise, in the following all catalysts studied have been immobilized with 25% surface coverage.

Systems designed earlier using an ethoxysilane linker could be recycled up to 13 times.^[4] As the record so far, a Wilkinson-type Rh catalyst immobilized recently *via* a phosphonium-bound rigid tetraphenyltin scaffold can be recycled 30 times until the H₂ consumption drops below 100% within 100 h.^[5b] Following the usual test protocol for new linker systems, we probed the first run of the catalysts **13i–15i**



Scheme 3. Catalytic hydrogenation of 1-dodecene; pressure 1.1 atm, substrate:catalyst ratio 100:1, reaction temperature: 60 °C, surface coverage of catalyst: *ca.* 2 metal centers per 100 nm².

in comparison with Wilkinson's catalyst in solution. Encouraged by the catalytic activity of other Rh norbornadienyl complexes with chelate ligands,^[35] we included **18i** with the shortest possible alkyl chains in this study. The graphic representation of the results in Figure 7 shows that according to expectation, the homogeneous catalyst $\text{ClRh}(\text{PPh}_3)_3$ is the fastest, because the substrate does not have to diffuse into the pores of a support material and contains triaryl- instead of diarylalkylphosphine ligands. Regarding the chain lengths of the linkers, the catalyst with the longest alkyl chain, **15i**, is the most active in the hydrogenation of 1-dodecene (Figure 7), probably due to its maximal mobility. It is followed by the C₇ species **14i**, and finally **13i**. In contrast to our anticipation, however, the catalyst **18i** that is bound to the surface *via* a tripod-type linker is only in the beginning the least active. After an induction period of about two hours, it catalyzes the hydrogenation even faster than **15i**, and reaches 100% substrate conversion at about the same overall reaction time (Figure 7). The ^{31}P MAS spectrum of **15i** after catalysis (Figure 6, *top*) shows basically the same signals as the spectrum recorded of the material prior to catalysis. Only the relative signal intensities are changed, a phenomenon observed previously.^[3c,4b] Most importantly, no signals of dimeric species of the type $[(\text{R}_3\text{P})_2\text{RhCl}]_2$ are visible.

Next, the recycling characteristics of all immobilized catalysts have been tested. In earlier findings for immobilized Wilkinson-type catalysts at room temperature,^[4] the first run had always shown the fastest conversion, and the activity slowly decreased with every subsequent batchwise recycling step. The catalysts **13i–15i** and **18i**, however, display a different scenario, as the first run is often comparatively slow (Figure 8). Then, the activity increases with every recycling step and reaches a maximum at the third or fourth run, before the activity finally consolidates at about 100%

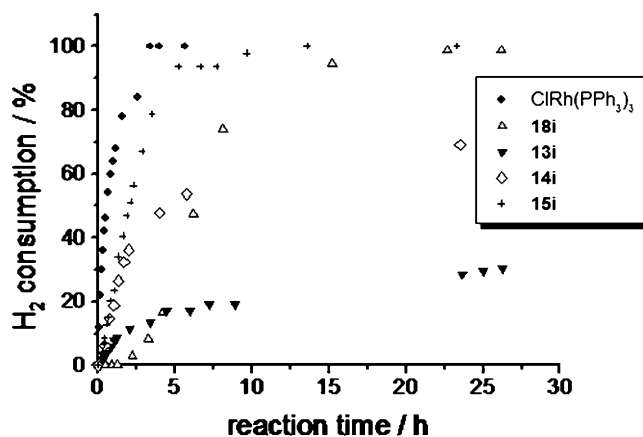


Figure 7. Activities of the indicated homogeneous and immobilized catalysts for the hydrogenation of 1-dodecene in the first run.

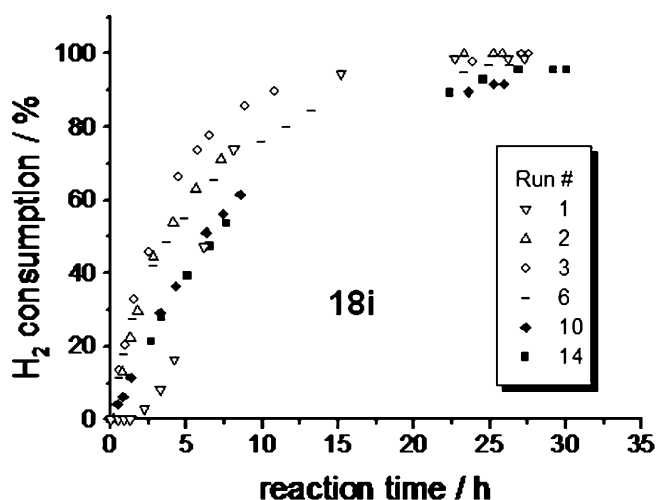


Figure 8. Hydrogen consumption during 14 batchwise catalytic runs using **18i**.

conversion within 30 to 40 h. For **18i** there is even an induction period of about two hours. These phenomena can be explained based on the catalysis results discussed below.

Interestingly, **18i** shows a better recycling characteristic than **13i**, although the alkyl chains of the linker are shorter. Catalyst **18i** can be recycled for a respectable 14 times, before the conversion no longer reaches 100% within 35 h (Figure 8). The catalyst **13i** can only be recycled 3 times, before the conversion drops below 85% within 120 h. End-capping of residual surface silanol groups after the linker tethering and prior to the catalyst immobilization with trimethylsilyl (TMS) groups improved the recycling characteristics of **13i** substantially. Now, **13i** can be recycled 7 times with 100% conversion of 1-dodecene within 35 h. Therefore, we conclude that with short linkers and in the absence of “shielding” counteranions (see X-ray structure in Figure 2), the decomposition of the catalytically active species by contact with the reactive silica surface is a major problem that can be ameliorated with TMS-capping. However, the increase in catalytic activity from the first run with only 70% conversion within 30 h to the third, fourth and consecutive runs with 100% indicates the formation of a second catalytically active species even after end-capping (see below).

In contrast to our expectation, based on the activity in the first run (Figure 7) and the fact that the catalyst **15i** incorporates the longest linker alkyl chains that are supposed to keep the catalyst at a distance from the surface, the recycling characteristics of **15i** are disappointing. In the second and third recycling run, **15i** needs about 100 h to reach 80% conversion. We interpret this scenario as an optimally mimicked homogeneous catalysis in the first run, while subsequently another, catalytically less active species is formed (see

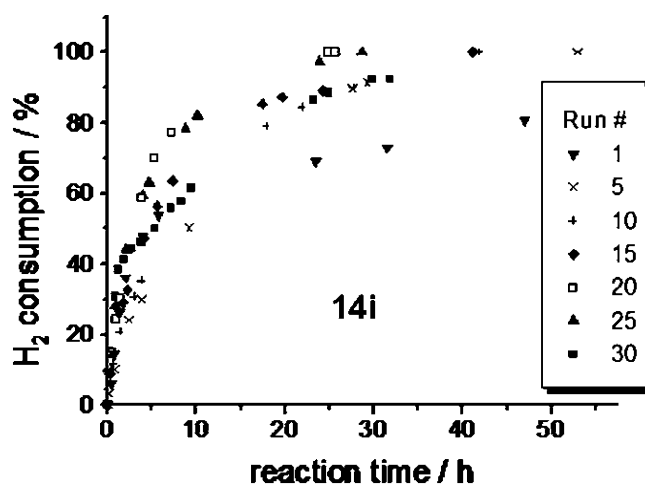


Figure 9. Hydrogen consumption during 30 batchwise catalytic runs using **14i**. Only every fifth run is shown for clarity.

below), or the catalyst decomposes partly by the interaction with the silica surface.

The most impressive recycling performance has been found for **14i**, which can be recycled for 30 times in a batchwise manner, before the conversion of 1-dodecene to dodecane drops below 100% within 50 h (Figure 9). Interestingly, between the batchwise recycling runs, the washed and dried immobilized catalyst can be stored under an inert gas atmosphere for months without losing activity, when the recycling experiments are resumed. Wilkinson-type Rh catalysts immobilized with other linker types are less robust in this respect.^[4b]

Encouraged by the positive effect of end-capping on **13i**, in order to further increase the activity and prolong the lifetime of **14i**, we attached TMS and triphenylsilyl groups on the silica surface after the immobilization of **11i**, and prior to the generation of **14i**. However, practically no change in the catalytic activity or lifetime of silyl-capped **14i** versus unmodified **14i** has been observed. Obviously, for **14i** a robust catalytic species is formed, whose performance is no longer dependent on the nature of the silica surface.

From the above results we conclude that there is at least one additional species, other than **13i**–**15i**, and **18i**, formed during catalysis, when we apply the new linkers. The most basic question in order to narrow in the nature of the new species is, whether the catalytic activity remains with the support, or whether it is found in solution now. In order to check this issue, a split test has been performed on **14i** (Figure 10). After about 8 h of the third catalytic run with **14i** and 40% conversion, an aliquot of the supernatant was removed from the reaction mixture. Then, the supported catalyst with the remaining supernatant, and also the aliquot of the supernatant, were subjected again to the hydrogenation conditions. While the solid re-

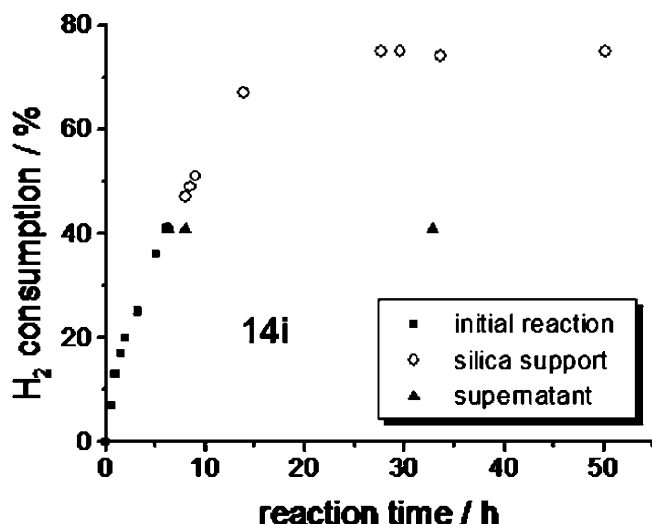


Figure 10. Split test to prove that no Rh species in solution, but only the surface-bound catalyst **14i** hydrogenates the substrate 1-dodecene (details see Experimental Section).

mains catalytically active and consumes all residual 1-dodecene, the supernatant does not show any substrate conversion (Figure 10). Therefore, we conclude that all catalytically active species involved stay firmly attached to the support.

Another test that confirms that the catalytically active species stays on the support involves covalently binding an olefin to a different batch of support material and checking whether it is hydrogenated by the immobilized catalyst.^[36] For this three-phase test, allyltriethoxysilane was covalently bound to a different batch of silica *via* Si–O–Si linkages according to the well-explored procedure.^[24b,c] Then, the batch with allyltriethoxysilane-modified silica was combined with a batch of **14i** and the hydrogenation procedure was started. The immobilized catalyst **14i** did not hydrogenate any of the tethered olefin, as checked by monitoring the hydrogen consumption (Figure 11) and ¹³C HR-MAS^[11a] of the tethered olefin. When, as a control experiment, the homogeneous catalyst ClRh(PPh₃)₃ (**1**) was added, however, all surface-bound allyl groups were hydrogenated. Therefore, we conclude that no catalytically active species leaches from **14i** into solution.

In order to better describe the new surface-bound catalyst that forms during the reaction, we took the following observation into account: In contrast to earlier hydrogenation scenarios,^[5b] here we also noticed that, with the new linker system, the silica-bound catalyst turned from orange to black already within 5 h during the first run. This indicates the formation of metal particles in addition to the molecular catalyst, and based on the pioneering work of Angelici et al.,^[37] this would explain the initial increase of the

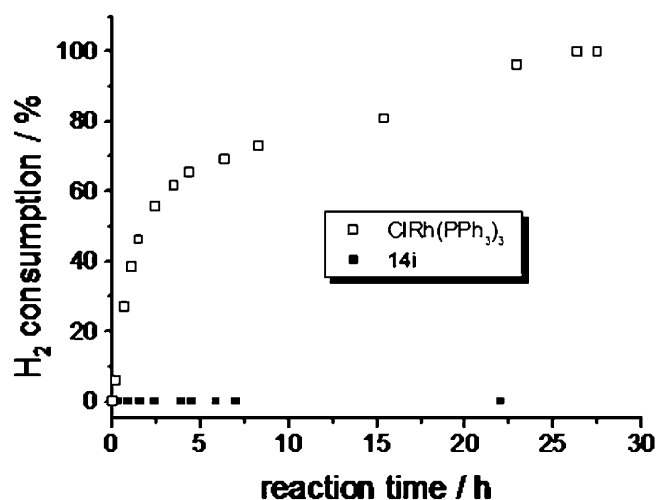


Figure 11. Three-phase test using immobilized allyltriethoxysilane (details see text and Experimental Section).

hydrogenation activity due to the spill-over effect of the metal particles.

In order to check, whether indeed metal particles form with our new linker system during catalysis, we performed a test developed by the Crabtree group.^[38] Homogeneous, molecular Rh catalysts can be poisoned by adding DBCOT (dibenzo[*a,e*]cyclooctatetraene) to the reaction mixture. DBCOT is a strong ligand, but is not hydrogenated. Therefore, once DBCOT binds to the Rh center, it prevents further hydrogenation of other substrates. However, DBCOT does not strongly bind to metal surfaces due to steric constraints. Therefore, it cannot inhibit the catalytic activity of metal particles.

Figure 12 shows the DBCOT poisoning results and the validity of the test. When two equivalents of

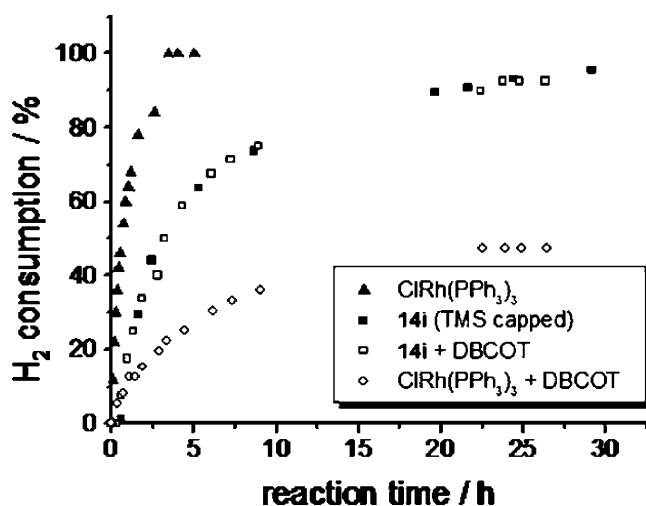


Figure 12. Hydrogen consumption of the shown catalysts with and without the poisoning agent DBCOT (dibenzo[*a,e*]cyclooctatetraene) (see text).

DBCOT are added to the homogeneous Wilkinson's catalyst in solution, the conversion of dodecene decreases from originally 100% within 4 h to about 43% in 25 h. For the test with the immobilized catalyst **14i**, one batch of TMS-capped **14i** at the 8th run has been studied. In comparison, **14i** at the 9th run has been tested in the presence of two equivalents of DBCOT. Both substrate consumption curves are nearly identical. Therefore we conclude that at the 8th catalytic run at the latest the catalyst consists mainly of metal particles that are not affected by the DBCOT, and not of molecular single-site species.

Next we studied whether the metal particle formation coincides with the catalyst turning black in the first run. For this purpose, fresh TMS-capped **14i** has been split into two batches, and one has been allowed to hydrogenate 1-dodecene under the standard conditions, while the other has been additionally poisoned with 2 equivalents of DBCOT. In the first 5 h both batches showed an orange color, and while the poisoned batch only reached about 30%, the pristine batch gave about 44% conversion (Figure 13). After 5 h, the poisoned catalyst turned black and its catalytic activity soon matched the one of the pristine batch. Therefore, we conclude that the formation of metal particles correlates with the color change of the catalyst, and that this takes place within the first 5 to 10 h of hydrogenation. So, in the beginning of the first catalytic run, both surface-bound molecular complexes, as well as metal particles take part in the catalytic hydrogenation.

For **18i** the extended induction period is most probably not due to the norbornadiene dissociation, because the molecular complex **18** in solution is not catalytically active. The catalytic activity of **18i** seems to

be solely based on the formation of metal particles, which coincides with the color change occurring with the onset of the hydrogen consumption.

Further evidence for this assumption is based on the selectivity of the hydrogenation reaction. It is known that heterogeneous catalysts that consist of metal particles can shift double bonds in linear 1-alkenes,^[39a] as well as cyclic olefins.^[39b] This double bond shift only takes place in the presence of H₂. For example, material containing Rh(0) on silica, obtained by depositing [(COD)RhCl]₂ on silica according to the literature procedure^[40] (see Experimental Section), did not isomerize 1-dodecene under the standard catalysis conditions, but in the absence of H₂, as proven by ¹H NMR. The same result was obtained for **18i** after the 14th run, when it was stirred with 1-dodecene under the standard conditions, but without H₂. Since this isomerization will not be obvious for 1-dodecene after quantitative hydrogenation, we investigated the reaction mixture of the third catalytic run by GC and ¹H NMR at about 40% conversion with catalyst **14i**. Indeed, not only resonances for the terminal olefin ¹H signals of residual 1-dodecene with a relative intensity of about 2%, but also ca. 98% of signal intensity for protons at different internal double bonds have been found. The reason why 1-dodecene is present in only 2% is most probably because it is more easily transformed into dodecane than the dodecene isomers with internal double bonds, and is therefore continually removed from the equilibrium. As a comparison, we checked the reaction mixture after 52% substrate conversion by Wilkinson's catalyst, and found less than 20% of ¹H signal intensity stemming from dodecene isomers with internal double bonds.

Finally, the nitrobenzene test^[38] has been applied to prove the presence of metal particles on the silica surface of catalyst **13i**. According to this test, only heterogeneous metal particles catalyze the reduction of nitrobenzene to aniline. Indeed, Wilkinson's catalyst in solution does not consume hydrogen in the presence of nitrobenzene within the first 10 h of reaction. Hydrogen consumption only starts when the solution turns black and cloudy, indicating decomposition of the homogeneous catalyst under formation of metal particles. Catalyst **13i**, after an induction period of about 10 h, starts to transform nitrobenzene into aniline, and achieves about 85% conversion after 200 h reaction time.

Next we sought to generate catalytically active metal particles to prove our hypothesis. The immobilized catalyst **14i** can be stirred at 70 °C under a nitrogen atmosphere overnight without a visible change of the orange color taking place. However, with admission of hydrogen, the color darkens slightly even at room temperature. At 70 °C, exposure of **14i** to a hydrogen atmosphere leads to the blackening of the material within one hour. Therefore, we conclude that

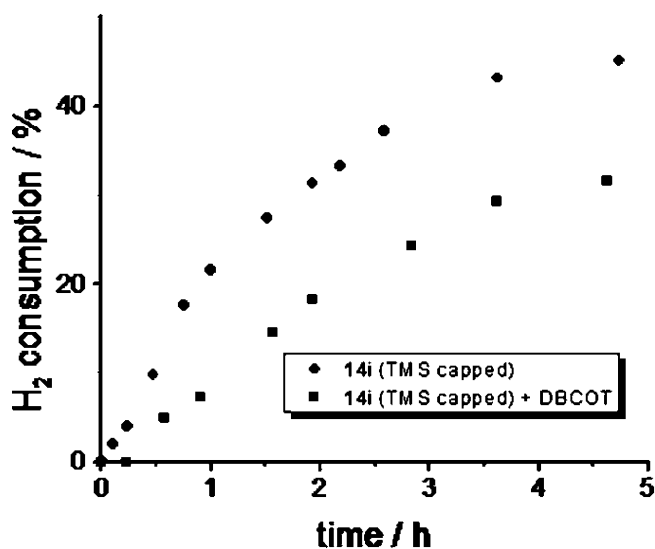


Figure 13. Hydrogen consumption of the TMS-capped catalyst **14i** in the first run with and without the poisoning agent DBCOT (dibenzo[*a,e*]cyclooctatetraene) (see text).

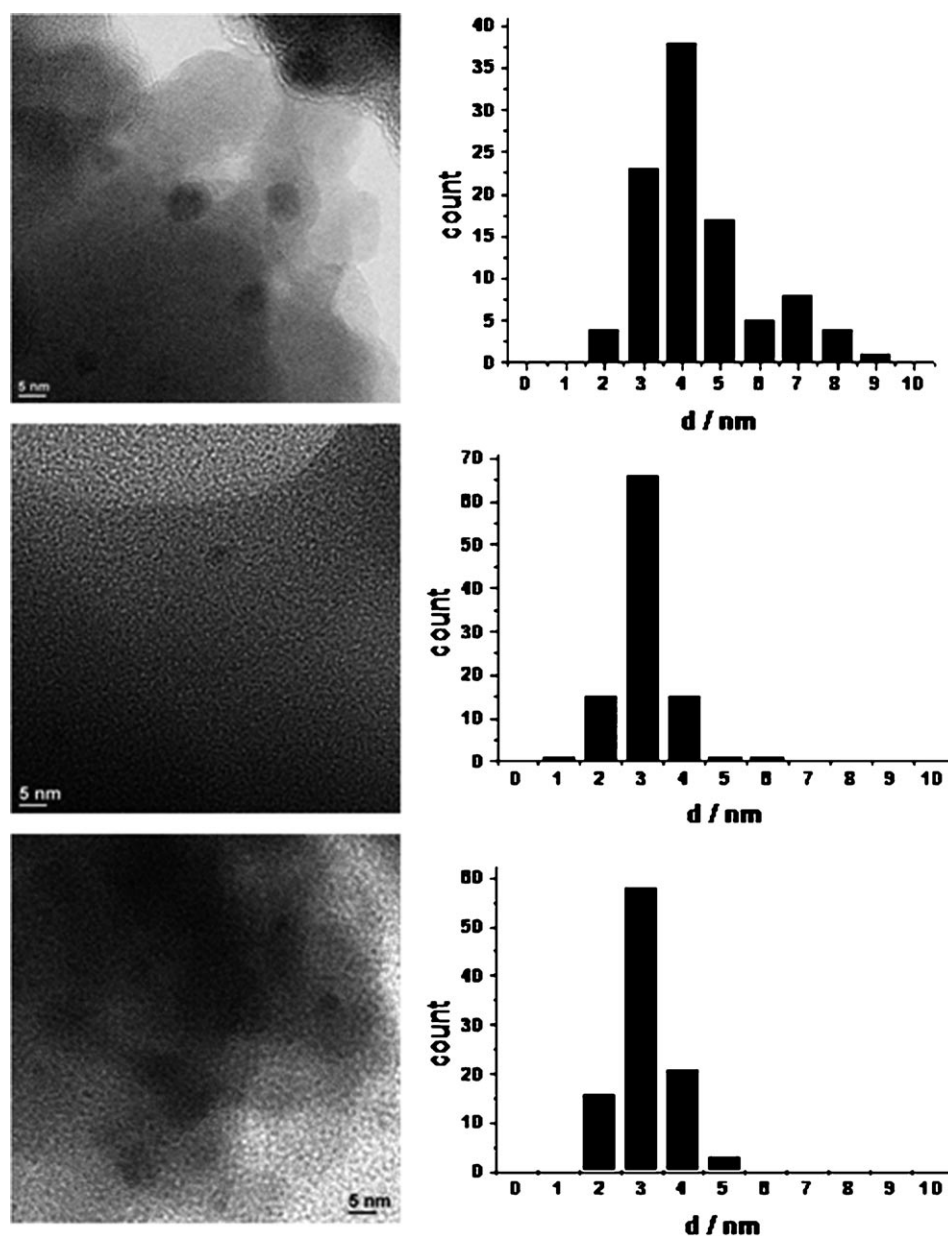


Figure 14. TEM images (*left*) of Rh nanoparticles that formed during catalysis with **13i** (*top*), **14i** (*middle*), and **15i** (*bottom*), and their corresponding size distributions (*right*).

hydrogen is the reducing agent, while the temperature is only a minor issue, and the olefin does not play a significant role in this process. Based on this insight, $[(\text{COD})\text{RhCl}]_2$ was deposited on silica according to the literature procedure^[40] (see Experimental Section), and the dry material was reduced in a stream of hydrogen, while increasing the temperature from 60 to 120 °C for 4 h. During this time, the color of the powder changed from yellow to black. The resulting material contains 0.04 weight% of Rh. The heterogeneous catalyst obtained in this way is rather slow with respect to hydrogenation. For about 85% conversion it needs 80 h. However, the recycling characteristics

are reasonable, as the activity does not change substantially between the second and the third runs. Interestingly, comparing the obtained hydrogen consumption curves with those of **15i**, they are nearly identical. Therefore, we conclude that due to the long linker alkyl chains that allow maximal mobility, interactions with the surface, and hydrogen access, **15i** is reduced rapidly and forms metal particles.

In order to confirm these assumptions and probe the sizes of the formed metal particles, we recorded TEM measurements of **13i–15i**. The pictures in Figure 14 show clearly that Rh nanoparticles^[41] form within the silica. Their size distribution is similar and

rather narrow, with an average diameter of 3 to 4 nm. The diameter is most probably dominated by the average pore size of the support material (4 nm), that prevents the particles from growing any larger. Therefore, the size distribution proves that the nanoparticles reside within the pores of the support material. The inclusion of the nanoparticles within the pores explains the optimal recyclability of the catalysts, and the absence of leaching. The formation of 100% nanoparticles from the starting immobilized catalysts is unlikely, since the ^{31}P solid-state NMR spectra of the materials before and after catalysis (Figure 6) are very similar. It is also noteworthy that no resonance for uncoordinated, surface-bound phosphines occurs. Unfortunately, the TEM measurements do not allow precise quantification of the Rh centers. However, clearly only a fraction of the metal centers is exposed on the surface and accessible for the substrate. But on the other hand, the longevity of the nanoparticle catalysts is yet another proof that the pores of the silica are not clogged by the substrate or products, or any decomposed catalyst.

Conclusions

Using a new trisphosphine chelate linker system we could obtain immobilized Rh catalysts that can be recycled more than 30 times without major loss of activity. It has been demonstrated that in contrast to previous Rh-catalyst systems that were immobilized *via* rigid tetraphenyl-element linker scaffolds that prevent interactions with the silica surface,^[5b] here due to the reducing effect of hydrogen, a second catalytically active species forms at the higher temperatures of 60 °C needed for these catalysts with alkyl-diphenylphosphine ligands to be active. It could be proven by catalytic test reactions, catalyst poisoning experiments, and TEM measurements that the new active species consist of Rh nanoparticles.^[41] All linkers lead, on a different time scale, basically to the same nanoparticles, explaining their very similar catalytic characteristics. Future work will be devoted to defining the process of nanoparticle formation quantitatively.

Experimental Section

General Remarks

The ^1H , ^{13}C , ^{19}F , and ^{31}P NMR spectra of liquids were recorded at 499.70, 125.66, 202.28, and 470.17 MHz on a 500 MHz Varian spectrometer. The ^{13}C , ^{19}F , and ^{31}P spectra were recorded with ^1H decoupling if not stated otherwise. The solid-state NMR spectra were measured with a Bruker Avance 400 widebore NMR spectrometer with 4 or 7 mm MAS probeheads. For the ^{31}P HR-MAS and MAS measure-

ments ^1H high-power decoupling was applied. The recycle delays were 5 s for HR-MAS and 10 s for MAS spectra. For more measurement details, see ref.^[11a] GC analyses were carried out on a Shimadzu GC 2010 gas chromatograph equipped with a SHRXI-5MS column (15 m \times 0.25 mm \times 0.25 μm) and a flame ionization detector (GC:FID). TEM images were obtained on an FEI Tecnai G2 F20 microscope and ImageJ software was used to determine the particle size distribution. All reactions were carried out using standard Schlenk techniques and a purified N_2 atmosphere, if not stated otherwise. Reagents purchased from Sigma Aldrich or VWR were used without further purification. Solvents were dried by boiling them over Na, distilled, and stored under N_2 . CH_2Cl_2 was obtained from a solvent purification system. The silica (Merck, 40 Å average pore diameter, 0.063 to 0.2 mm average particle size, specific surface area 750 m^2g^{-1}) was rigorously dried under vacuum at 400 °C for 4 days to remove adsorbed water and condense surface silanol groups. Ligand **3** has been synthesized according to the procedure given by Clark and Hartwell,^[12a] the phosphines **4** and **5** as described by Gladysz.^[14]

General Procedure for the Immobilization of Phosphine Linkers 10–12 and 17, and Rh Complex 18 *via* the Phosphonium Group

Phosphine linker **11** (67 mg, 0.065 mmol) was dissolved in toluene (15 mL) and added to a suspension of 2.434 g of SiO_2 in toluene (40 mL). The mixture was stirred overnight at 50 °C. The silica was allowed to settle down and the supernatant was removed. The functionalized silica **11i** was then washed with toluene (2 \times 10 mL) and with Et_2O (2 \times 10 mL). Subsequently the silica was dried under vacuum for several hours. The supernatant and the solvents from the washing process were combined and all volatile matter was removed under vacuum. The residue showed no ^{31}P NMR resonance, so all the linker **11** was immobilized on the support, resulting in **11i** with about 2 molecules per 100 nm^2 of silica surface (data for all immobilized species are given in Table 1).

General Procedure for the Catalyst Preparation

$\text{ClRh}(\text{PPh}_3)_3$ (23 mg, 0.025 mmol), dissolved in 10 mL of toluene, was added to a slurry of the functionalized silica **11i** (1.006 g, 0.026 mmol ligand) in 10 mL of toluene. The mixture was stirred overnight at room temperature, then the silica was allowed to settle down and the supernatant was removed. The catalyst-containing silica **14i** was washed with toluene (3 \times 10 mL) and dried under vacuum for 4 h. The supernatant and the washing portions were combined and the solvent was removed under vacuum. The residue was analyzed by NMR and showed only the ^{31}P resonance of PPh_3 .

General Procedure for TMS-Capped Catalysts

To prepare catalyst **14i-TMS** with end-capped SiOH groups, ligand **11** was protected as the BH_3 adduct by adding BH_3SMe_2 (0.5 mL, 400 mg, 5.265 mmol) to a solution of **11** (240 mg, 0.235 mmol) in toluene (20 mL). The reaction mixture was stirred for 5 h at room temperature and the quantitative conversion to **11BH₃** was checked by ^{31}P NMR (broad signal, $\delta = 15.5$ ppm). Then the solvent was removed

under vacuum and the precipitate washed with pentane (2×5 mL). **11-BH₃** was then immobilized according to the general procedure described above. 4 mL of Me₃SiOEt were added to **11i-BH₃** (2.999 g, 0.080 mmol ligand) and the mixture was stirred at 60 °C for 40 h. Then the supernatant was removed and the functionalized silica was washed with toluene (3×10 mL) and dried under vacuum. Then **11i-BH₃-TMS** was added to 139 mg (1.239 mmol) of DABCO (1,4-diazabicyclo[2.2.2]octane), dissolved in 30 mL of toluene, and stirred overnight. Finally, the supernatant was removed, and **11i-TMS** was washed two times with 10 mL aliquots of toluene. Then **14i-TMS** was prepared from **11i-TMS** according to the general procedure for the catalyst preparation described above.

General Procedure for the Catalytic Hydrogenation

The immobilized catalyst **14i** (386 mg, 0.010 mmol Rh) was added to 4 mL of toluene in a Schlenk flask. Then the Schlenk flask was attached to the standardized hydrogenation apparatus^[4c] and warmed up to 60 °C. The apparatus was allowed to stand under H₂ prior to catalysis in order to make sure that H₂ is not lost due to a leakage. Additionally, any loss of H₂ after 100% conversion of the substrate was monitored and excluded. To start the catalysis, 1 mmol of 1-dodecene, dissolved in 1 mL of toluene, was added to the suspension through the stopcock *via* syringe. Then the suspension was stirred vigorously with a magnetic stir bar and the hydrogen uptake was monitored. After complete consumption of the hydrogen the silica was allowed to settle down, the supernatant was removed and the silica was washed with toluene (2×4 mL). The supernatant was analyzed by GC and ¹H NMR to confirm quantitative conversion of the olefin to dodecane. The H₂ consumption always matched the substrate formation within the error margins of the analytical methods. For example, after the consumption of 54% H₂ in the 15th catalytic run with **14i**, the GC and ¹H NMR analyses indicated 57 and 55% dodecane formation.

Procedure for the Three-Phase Test

Immobilized catalyst **14i-TMS** (375 mg, 0.01 mmol Rh) and allyltrioxyethyl-functionalized silica^[24] (890 mg, 0.5 mmol allyl groups) were added to a Schlenk flask with 5 mL of toluene and warmed to 60 °C. Then the Schlenk flask was purged with H₂, connected to the standardized hydrogenation apparatus^[4c] and the H₂ consumption was monitored. As a control experiment the same procedure was carried out with Wilkinson's catalyst (8 mg, 0.01 mmol) instead of immobilized catalyst **14i-TMS**.

Procedure for the Split Test

Immobilized catalyst **14i** (386 mg, 0.010 mmol Rh) was added to 4 mL of toluene in a Schlenk flask. Then the Schlenk flask was attached to the standardized hydrogenation apparatus^[4c] and warmed to 60 °C. To start the catalysis 1-dodecene (1 mmol, dissolved in 1 mL of toluene) was added. The hydrogen consumption was monitored and after *ca.* 40% conversion the hydrogen reservoir was disconnected and the silica support was allowed to settle down. Then 2 mL of the hot supernatant were removed with a syringe

and filtered through a frit. Both the remaining reaction mixture with the silica support and the filtered supernatant were reconnected to separate hydrogenation apparatuses, and the hydrogen consumption was monitored for both samples. After the hydrogen uptake had stopped, for both cases the reaction mixtures were analyzed by GC and ¹H NMR.

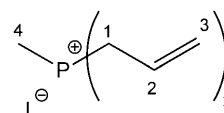
General Procedure for the Rh(0) Catalyst Preparation^[40]

Silica (1.029 g) was suspended in 15 mL of toluene. [(COD)RhCl]₂ (10 mg, 0.020 mmol) was dissolved in 10 mL of toluene, added to the silica slurry, and the mixture was stirred for 3 h at room temperature. Then the solvent was removed under vacuum to give a yellow powder. This material was then heated from 60 °C to 120 °C over 4 h in an H₂ gas stream. The material darkened gradually until it became black.

Catalyst Poisoning Experiment with DBCOT

The immobilized catalyst **14i-TMS** (375 mg, 0.010 mmol Rh) was stirred in 4 mL of toluene in a Schlenk flask. Then dibenzo[*a,e*]cyclooctatetraene DBCOT (4 mg, 0.020 mmol) was added and the mixture was stirred for 2 h at room temperature. The Schlenk flask was attached to the standardized hydrogenation apparatus^[4c] and warmed to 60 °C. Then 1 mmol of 1-dodecene, dissolved in 1 mL of toluene, was added to the slurry through the stopcock *via* syringe. While the mixture was stirred, the hydrogen uptake was monitored. After complete conversion the silica was allowed to settle down. Then the supernatant was removed and the silica was washed with toluene (2×4 mL). The supernatant was analyzed by GC and ¹H NMR to confirm 100% conversion.

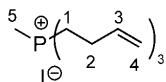
Methyltris(prop-2-enyl)phosphonium Iodide (6)



PCl₃ (254 mg, 1.849 mmol) was dissolved in Et₂O (10 mL) and added dropwise to a 1 M ether solution of allylmagnesium bromide (5.5 mL, 5.500 mmol), diluted with 40 mL in Et₂O, over 1 h at 0 °C. Then the reaction mixture was allowed to warm up to room temperature and stirred overnight. After the reaction mixture was cooled to 0 °C and quenched with 20 mL of H₂O, the mixture was stirred at room temperature for 2 h. The organic layer was filtered through Na₂SO₄ and the aqueous layer was washed twice with 30 mL portions of Et₂O. The organic layers were combined, 947 mg (6.672 mmol) of methyl iodide was added, and the reaction mixture was stirred overnight at room temperature. Then the solvent was removed under vacuum. The crude product was washed with pentane (6×15 mL) to give triallyl(methyl)phosphonium iodide as a colorless waxy solid; yield: 263 mg (0.977 mmol, 53%). ¹H NMR (CDCl₃, 499.70 MHz): δ = 5.70–5.87 (m, 3H, H-2), 5.58 [ddq, ³J_{trans}(H-1H) = 16.9 Hz, ³J(H-1H) = 5.3 Hz, ²J(H-1H) = 1.0 Hz,

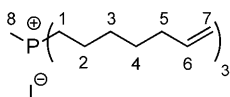
3H, H-3_Z], 5.49 [ddd, $^3J_{cis}(^1H-^1H)=9.9$ Hz, $^3J(^1H-^1H)=4.8$ Hz, $^2J_{cis}(^1H-^1H)=0.8$ Hz, 3H, H-3_E], 3.52 [dd, $^2J(^{31}P-^1H)=15.8$ Hz, $^3J(^1H-^1H)=7.4$ Hz, H-1], 2.08 [d, $^2J(^{31}P-^1H)=13.2$ Hz, 3H, H-4]; ^{13}C NMR (CDCl₃, 125.66 MHz): $\delta=125.32$ [d, $^3J(^{31}P-^{13}C)=12.2$ Hz, C-2], 123.17 [d, $^2J(^{31}P-^{13}C)=10.3$ Hz, C-3], 25.72 [d, $^1J(^{31}P-^{13}C)=47.7$ Hz, C-1], 4.14 [d, $^1J(^{31}P-^{13}C)=53.3$ Hz, C-4]; ^{31}P NMR (CDCl₃, 202.28 MHz): $\delta=27.47$.

Methyltris(but-3-enyl)phosphonium Iodide (7)



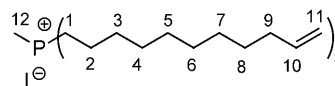
Phosphine **4** (311 mg, 1.584 mmol) was dissolved in 20 mL of toluene and 0.43 mL of CH₃I (800 mg, 5.654 mmol) was added. The reaction mixture was stirred at room temperature for 48 h. Then the solvent was removed under vacuum and the remaining residue was washed with pentane to give **7** as a colorless solid; yield: 401 mg (1.185 mmol, 75%). 1H NMR (CDCl₃, 499.70 MHz): $\delta=5.88$ [ddt, $^3J_{trans}(^1H-^1H)=16.6$ Hz, $^3J_{cis}(^1H-^1H)=10.2$ Hz, $^3J(^1H-^1H)=6.4$ Hz, 3H, H-3], 5.23 [ddt, $^3J_{trans}(^1H-^1H)=17.1$ Hz, $^2J(^1H-^1H)=2.1$ Hz, $^4J(^1H-^1H)=1.5$ Hz, 3H, H-4_{cis}], 5.16 [ddt, $^3J_{cis}(^1H-^1H)=10.2$ Hz, $^2J(^1H-^1H)=2.3$ Hz, $^4J(^1H-^1H)=1.2$ Hz, 3H, H-4_{trans}], 2.67 (m, 6H, H-1), 2.46 (m, 6H, H-2), 2.02 [d, $^2J(^{31}P-^1H)=13.5$ Hz, 3H, H-5]; ^{13}C NMR (CDCl₃, 125.66 MHz): $\delta=134.75$ [d, $^3J(^{31}P-^{13}C)=12.3$ Hz, C-3], 117.97 (s, C-4), 25.82 [d, $^2J(^{31}P-^{13}C)=4.1$ Hz, C-2], 20.53 [d, $^1J(^{31}P-^{13}C)=47.8$ Hz, C-1], 6.43 [d, $^1J(^{31}P-^{13}C)=50.9$ Hz, C-5]; ^{31}P NMR (CDCl₃, 202.28 MHz): $\delta=33.28$ (s); melting range 170–173 °C.

Methyltris(hept-6-enyl)phosphonium Iodide (8)



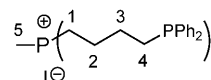
Phosphine **5** (362 mg, 1.123 mmol) was dissolved in 30 mL of toluene and 0.3 mL of CH₃I (684 mg, 4.819 mmol) was added. The reaction mixture was stirred at room temperature for 36 h. Then the solvent was removed under vacuum and the remaining residue was washed with pentane to give **8** as a colorless oil; yield: 356 mg (0.766 mmol, 68%). 1H NMR (C₆D₆, 499.70 MHz): $\delta=5.89$ [tdd, $^3J_{trans}(^1H-^1H)=16.9$, 3 Hz, $^3J_{cis}(^1H-^1H)=10.1$ Hz, $^3J(^1H-^1H)=6.7$, 3 Hz, 3H, H-6], 5.17 [ddt, $^3J_{trans}(^1H-^1H)=17.1$ Hz, $^2J(^1H-^1H)=2.1$ Hz, $^4J(^1H-^1H)=1.5$ Hz, 3H, H-7_{cis}], 5.07 [tdd, $^3J_{cis}(^1H-^1H)=10.2$ Hz, $^2J(^1H-^1H)=2.3$ Hz, $^4J(^1H-^1H)=1.2$, 3 Hz, 3H, H-7_{trans}], 2.39–2.56 (m, 6H, H-1), 2.19 [d, $^2J(^{31}P-^1H)=13.8$ Hz, 3H, H-8], 2.04–2.16 (m, 6H, H-5), 1.41 (b, 18H, H-2, H-3, H-4); ^{13}C NMR (C₆D₆, 125.66 MHz): $\delta=139.05$ (s, C-6), 114.98 (s, C-7), 33.94 (s, C-5), 30.89 [d, $^3J(^{31}P-^{13}C)=15.4$ Hz, C-3], 28.61 (s, C-4), 21.90 [d, $^2J(^{31}P-^{13}C)=4.5$ Hz, C-2], 20.83, [d, $^1J(^{31}P-^{13}C)=48.2$ Hz, C-1], 5.87 [d, $^1J(^{31}P-^{13}C)=51.5$ Hz, C-8]; ^{31}P NMR (C₆D₆, 202.28 MHz): $\delta=29.69$ (s).

Methyltris(undec-10-enyl)phosphonium Iodide (9)



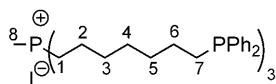
Phosphine **6** (431 mg, 0.878 mmol) was dissolved in 20 mL of toluene and 463 mg of CH₃I (0.203 mL, 3.272 mmol) was added. The reaction mixture was stirred at room temperature for 24 h. Then the solvent was removed under vacuum and the remaining residue was washed with pentane to give **9** as a colorless oil; yield: 490 mg (0.774 mmol, 88%). 1H NMR (C₆D₆, 499.70 MHz): $\delta=5.82$ [ddt, $^3J_{trans}(^1H-^1H)=15.0$ Hz, $^3J_{cis}(^1H-^1H)=10.2$ Hz, $^3J(^1H-^1H)=6.7$ Hz, 3H, H-10], 4.96–5.14 (m, 6H, overlapping H-11_{cis} and H-11_{trans}), 2.45–2.60 (m broad, 6H, H-1), 2.33 [d, $^1J(^{31}P-^1H)=13.8$ Hz, 3H, H-12], 2.07 (q, $J=7.3$ Hz, 6H, H-2*), 1.94–2.05 (m, 6H, H-9*), 1.20–1.51 (b, 36H, H-3, H-4, H-5, H-6, H-7, H-8); ^{13}C NMR (C₆D₆, 125.66 MHz): $\delta=139.26$ (s, C-10), 114.58 (s, C-11), 34.29 (s, C-9), 31.11 [d, $^3J(^{31}P-^{13}C)=15.1$ Hz, C-3], 29.99[#] (s), 29.93[#] (s), 29.56[#] (s), 29.43[#] (s), 22.17 [d, $^2J(^{31}P-^{13}C)=4.6$ Hz, C-2], 20.96 [d, $^1J(^{31}P-^{13}C)=48.5$ Hz, C-1], 6.09 [d, $^1J(^{31}P-^{13}C)=51.4$ Hz, C-12]; ^{31}P NMR (C₆D₆, 202.28 MHz): $\delta=31.11$ (s) (* assignments interchangeable, [#] no assignments of C-4 to C8 possible).

Methyltris(4-diphenylphosphinobutyl)phosphonium Iodide (10)



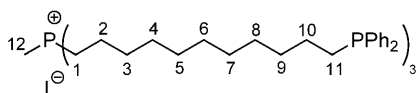
Phosphonium salt **7** (246 mg, 0.727 mmol), AIBN (119 mg, 0.724 mmol), and 0.9 mL of Ph₂PH (963 mg, 5.172 mmol) were combined in a Schlenk flask, heated under an N₂ atmosphere to 70 °C and stirred for 3.5 days. The conversion was monitored by ^{31}P NMR of the reaction mixture. After completion of the reaction, 2 mL of toluene were added to remove excess Ph₂PH, and the product precipitated after adding 3 mL of pentane. The supernatant was discarded and the solid was again treated with 2 mL of toluene and precipitated with 3 mL of pentane. The precipitate was dried under vacuum at 70 °C to give **10** as a colorless powder; yield: 640 mg (0.725 mmol, quantitative). 1H NMR (CDCl₃, 499.70 MHz): $\delta=7.42$ –7.37 (m, 12H, H_a), 7.34–7.28 (m, 18H, H_b, H_m), 2.31 (m, 6H, H-1), 2.09 (m, 6H, H-3), 1.95 [d, $^2J(^{31}P-^1H)=13.3$, 3H, H-5], 1.65–1.55 (m, 12H, overlapping H-2, H-4); ^{13}C NMR (CDCl₃, 125.66 MHz): $\delta=137.99$ [d, $^1J(^{31}P-^{13}C)=12.4$ Hz, C_j], 132.72 [d, $^2J(^{31}P-^{13}C)=18.65$ Hz, C_o], 128.81 (s, C_p), 128.58 [d, $^3J(^{31}P-^{13}C)=6.79$ Hz, C_m], 27.06 [d, $^1J(^{31}P-^{13}C)=12.6$ Hz, C-4], 26.85 [dd, $^2J(^{31}P-^{13}C)=16.8$ Hz, $^3J(^{31}P-^{13}C)=15.6$ Hz, C-3], 22.59 [dd, $^3J(^{31}P-^{13}C)=13.0$ Hz, $^2J(^{31}P-^{13}C)=4.3$ Hz, C-2], 20.45 [d, $^1J(^{31}P-^{13}C)=48.3$ Hz, C-1], 5.49 [d, $^1J(^{31}P-^{13}C)=51.9$ Hz, C-5]; ^{31}P NMR (C₆D₆, 202.28 MHz): $\delta=31.56$ (s, R₃MeP⁺), –16.49 (s, RPh₂P). The material is softening over the temperature range of 50–70 °C. HR-MS (MALDI⁺): $m/z=769.4390$, calcd. for C₄₉H₅₇P₄ [M⁺]; 769.3411; 785.4048, calcd. for C₄₉H₅₇P₄O [MO⁺]; 785.3360; 801.4435, calcd. for C₄₉H₅₇P₄O₂ [MO₂⁺]; 801.3309; 817.4487, calcd. for C₄₉H₅₇P₄O₃ [MO₃⁺]; 817.3258.

Methyltris(7-diphenylphosphinoheptyl)phosphonium Iodide (**11**)



Phosphonium salt **8** (442 mg, 0.952 mmol), AIBN (155 mg, 0.944 mmol), and 1.0 mL of Ph₂PH (1007 mg, 5.323 mmol) were combined in a Schlenk flask, heated under an N₂ atmosphere to 70 °C and stirred for 3.5 days. The conversion was monitored by ³¹P NMR of the reaction mixture. After completion of the reaction 2 mL of toluene were added to remove excess Ph₂PH, and the product precipitated after adding 3 mL of pentane. The supernatant was discarded and the solid was again treated with 2 mL of toluene and precipitated with 3 mL of pentane. The precipitate was dried under vacuum at 70 °C to give **11** as a colorless oil; yield: 971 mg (0.950 mmol, quantitative). ¹H NMR (C₆D₆, 499.70 MHz): δ = 7.52 [dd, ³J(³¹P-¹H) = 7.6 Hz, ³J(¹H-¹H) = 7.6 Hz, 12H, H_o], 7.14 [t, ³J(¹H-¹H) = 7.3 Hz, 12H, H_m], 7.07 [t, ³J(¹H-¹H) = 7.4 Hz, 6H, H_p], 2.47 (m, 6H, H-1), 2.32 [d, ²J(³¹P-¹H) = 13.9 Hz, 3H, H-8], 2.09 (m, 6H, H-6), 1.53 (m, 6H, H-7), 1.48–1.20 (m, 24H, H-2, H-3, H-4, H-5); ¹³C NMR (C₆D₆, 125.66 MHz): δ = 139.98 [d, ¹J(³¹P-¹³C) = 14.5 Hz, C_j], 133.24 [d, ²J(³¹P-¹³C) = 18.5 Hz, C_o], 128.79 [d, ³J(³¹P-¹³C) = 6.5 Hz, C_m], 128.65 (s, C_p), 31.26 [d, ¹J(³¹P-¹³C) = 12.7 Hz, C-3*], 30.89 [d, ¹J(³¹P-¹³C) = 15.1 Hz, C-5*], 29.05 (s, C-4), 28.59 [d, ¹J(³¹P-¹³C) = 12.5 Hz, C-6*], 26.47 [d, ¹J(³¹P-¹³C) = 16.3 Hz, C-7*], 22.10 [d, ²J(³¹P-¹³C) = 4.6 Hz, C-2], 20.86 [d, ¹J(³¹P-¹³C) = 47.9 Hz, C-1], 6.01 [d, ¹J(³¹P-¹³C) = 51.56 Hz, C-8]; ³¹P NMR (C₆D₆, 202.28 MHz): δ = 31.34 (s, R₃MeP⁺), -16.34 (s, RPh₂P) (* assignments interchangeable); HR-MS (MALDI⁺): *m/z* = 895.5497, calcd. for C₅₈H₇₅P₄ [M⁺]: 895.4819; 911.5306, calcd. for C₅₈H₇₅P₄O [MO⁺]: 911.4768; 927.5779, calcd. for C₅₈H₇₅P₄O₂ [MO₂⁺]: 927.4718.

Methyltris(11-diphenylphosphinoundecyl)phosphonium Iodide (**12**)



Phosphonium salt **9** (507 mg, 0.801 mmol), AIBN (130 mg, 0.792 mmol), and Ph₂PH (0.9 mL, 963 mg, 5.172 mmol) were combined in a Schlenk flask, heated under an N₂ atmosphere to 70 °C and stirred for 4 d. The conversion was monitored by ³¹P NMR of the reaction mixture. After completion of the reaction 2 mL of toluene were added to remove excess Ph₂PH, and the product precipitated after adding 3 mL of pentane. The supernatant was discarded and the solid was again treated with 2 mL of toluene and precipitated with 3 mL of pentane. The precipitate was dried under vacuum at 70 °C to give **12** as a colorless oil; yield: 940 mg (0.789 mmol, quantitative). ¹H NMR (C₆D₆, 499.70 MHz): δ = 7.48 [dd, ³J(³¹P-¹H) = 7.7 Hz, ³J(¹H-¹H) = 7.6 Hz, 12H, H_o], 7.16–7.05 (m, 18H, H_m, H_p), 2.53 (m, 6H, H-1), 2.33 [d, ²J(³¹P-¹H) = 13.8 Hz, 3H, H-12], 2.02 (m, 6H, H-10), 1.54 (m, 6H, H-11), 1.49–1.21 (m, 48H, H-2, H-3, H-4, H-5, H-6,

H-7, H-8, H-9); ¹³C NMR (C₆D₆, 125.66 MHz): δ = 140.03 [d, ¹J(³¹P-¹³C) = 14.7 Hz, C_j], 133.16 [d, ²J(³¹P-¹³C) = 18.6 Hz, C_o], 128.71 [d, ³J(³¹P-¹³C) = 6.4 Hz, C_m], 128.63 (s, C_p), 31.69 [d, ³J(³¹P-¹³C) = 12.7 Hz, C-9*], 31.14 [d, ³J(³¹P-¹³C) = 15.0 Hz, C-3], 30.11 (s, C-4[#]), 30.07 (s, C-5[#]), 29.98 (s, C-6[#]), 29.79 (s, C-7[#]), 29.61 (s, C-8[#]), 28.67 [d, ²J(³¹P-¹³C) = 12.5 Hz, C-10*], 26.56 [d, ¹J(³¹P-¹³C) = 16.4 Hz, C-11*], 22.19 [d, ²J(³¹P-¹³C) = 4.7 Hz, C-2], 20.93 [d, ¹J(³¹P-¹³C) = 48.2 Hz, C-1], C-12 signal not localized; ³¹P NMR (C₆D₆, 202.28 MHz): δ = 31.37 (s, R₃MeP⁺), -16.32 (s, RPh₂P) (*, # assignments interchangeable); HR-MS (MALDI⁺): *m/z* = 1063.6920, calcd. for C₇₀H₉₉P₄ [M⁺]: 1063.6697; 1079.6873, calcd. for C₇₀H₉₉P₄O [MO⁺]: 1079.6646; 1095.7205, calcd. for C₇₀H₉₉P₄O₂ [MO₂⁺]: 1095.6596.

Methyltris(diphenylphosphinomethyl)phosphonium Triflate (**17**)

Phosphine **16** (868 mg, 1.382 mmol) was dissolved in 50 mL of toluene and MeOTf (227 mg, 1.383 mmol), dissolved in 10 mL of toluene, was added dropwise over a period of 3 h. Then the reaction mixture was stirred overnight at room temperature. The product precipitated after adding 30 mL of pentane to the reaction mixture. The supernatant was removed and the precipitate was washed with pentane (2 × 10 mL), and subsequently with 50 mL of degassed H₂O. The residue was dried under vacuum to give **17** as a colorless powder; yield: 709 mg (0.894 mmol, 65%). Single crystals suitable for X-ray structure determination were grown from a solution in MeCN by slow evaporation of the solvent. ¹H NMR (C₆D₆, 499.70 MHz): δ = 7.45–7.40 (m, 12H, H_{ortho}), 7.38–7.35 (m, 18H, H_{meta}, H_{para}), 2.99 [d, ²J(³¹P-¹H) = 14.4 Hz, 6H, CH₂], 1.33 [d, ²J(³¹P-¹H) = 14.4 Hz, 3H, CH₃]; ¹³C-³¹P NMR (C₆D₆, 125.66 MHz): δ = 134.85 (C_j), 133.00 (C_o), 130.37 (C_p), 129.32 (C_m), 21.73 (CH₂), 8.48 (CH₃); ³¹P NMR (C₆D₆, 202.28 MHz): δ = 35.16 [q, ²J(³¹P-³¹P) = 54.3 Hz, R₃MeP⁺], -29.41 [d, ²J(³¹P-³¹P) = 54.5 Hz, RPh₂P]; ¹⁹F NMR (CDCl₃, 470.17 MHz): δ = -78.13 (CF₃); melting range 161–165 °C.

Rhodium Complex **18**

Ligand **17** (36 mg, 0.045 mmol) was dissolved in 4 mL of CH₂Cl₂ under an N₂ atmosphere. Then [Rh(nbd)₂]PF₆ (20 mg, 0.046 mmol), dissolved in 2 mL of CH₂Cl₂, was added. The reaction mixture was stirred for 30 min at room temperature, before the solvent was removed under vacuum and an orange powder was obtained. The residue was washed with pentane (2 × 5 mL) and dried under vacuum to give **18** as an orange powder; yield: 52 mg (0.54 mmol, quantitative). Single crystals suitable for X-ray structure determination were obtained by applying a pentane layer over a saturated solution of **18** in CH₂Cl₂. ¹H NMR (C₆D₆, 499.70 MHz): δ = 7.37 [t, ³J(¹H-¹H) = 7.4 Hz, 6H, H_p], 7.17 [t, ³J(¹H-¹H) = 7.4 Hz, 12H, H_m], 7.05 [broad t, ³J(³¹P-¹H) = 8.3 Hz, ³J(¹H-¹H) = 7.7 Hz, 12H, H_o], 3.84 (s, 2H, CH), 3.64 (s, 4H, =CH), 3.48 [d, ²J(³¹P-¹H) = 11.4 Hz, 6H, PCH₂], 2.69 [d, ²J(³¹P-¹H) = 14.3 Hz, 3H, CH₃], 1.46 (s, 2H, CH₂); ¹³C-³¹P NMR (C₆D₆, 125.66 MHz): δ = 143.67 (=CH), 133.25 (C_j), 132.03 (C_o), 131.61 (C_p), 129.82 (C_m), 75.60 (CH₂), 63.00 [d, ¹J(¹⁰³Rh-¹³C) = 3.3 Hz, =CH*], 50.45 [d, ²J(¹⁰³Rh-¹³C) = 5.8 Hz, PCH₂*], 46.6 (CH), 19.36 (CH₃); ³¹P NMR (C₆D₆, 202.28 MHz): δ = 38.88 [dq, ²J(³¹P-³¹P) =

21.3 Hz, $^3J(^{103}\text{Rh}-^{31}\text{P})=7.8$ Hz, R_3MeP^+], 7.19 [d, $^1J(^{103}\text{Rh}-^{31}\text{P})=118.3$ Hz, $^2J(^{31}\text{P}-^{31}\text{P})=21.2$ Hz, RPh_2P], -145.00 [sept, $^1J(^{31}\text{P}-^{19}\text{F})=712.5$ Hz, PF_6^-]; ^{19}F NMR (CDCl_3 , 470.17 MHz): $\delta=-71.38$ [d, $^1J(^{31}\text{P}-^{19}\text{F})=712.5$ Hz, PF_6^-], -78.71 (CF_3) (* assignments interchangeable).

Acknowledgements

We thank The Welch Foundation (A-1706) and NSF (CHE-0911207) for financial support. The FE-SEM acquisition was supported in part by the National Science Foundation under Grant No. DBI-0116835, and we thank Dr. Z. Luo of the Microscopy and Imaging Center (MIC) of Texas A&M University for the measurements. We thank Prof. Dr. G. Helmchen for a sample of DBCOT.

References

- a) K. C. Nicolaou, R. Hanco, W. Hartwig, (Eds.), *Handbook of Combinatorial Chemistry*, Wiley-VCH, Weinheim, Germany, **2002**, Vols. 1 and 2; b) W. Bannworth, E. Felder, (Eds.), *Combinatorial Chemistry*, Wiley-VCH, Weinheim, Germany, **2000**; c) J. A. Gladysz, (Ed.), *Recoverable Catalysts and Reagents*, Special Issue of *Chem. Rev.* **2002**, 102; d) J. Blümel, *Coord. Chem. Rev.* **2008**, 252, 2410–2423; e) F. R. Hartley, *Supported Metal Complexes*, D. Reidel Publ. Co., Dordrecht, The Netherlands, **1985**; f) D. E. DeVos, I. F. J. Vankelecom, P. A. Jacobs, (Eds.), *Chiral Catalyst Immobilization and Recycling*, Wiley-VCH, Weinheim, **2000**; g) G. Rothenberg, *Catalysis: Concepts and Green Applications*, Wiley-VCH, Weinheim, **2008**.
- a) E. F. Vansant, P. VanDer Voort, K. C. Vrancken, *Characterization and Chemical Modification of the Silica Surface*, Elsevier, Amsterdam, **1995**; b) R. P. W. Scott, *Silica Gel and Bonded Phases*, John Wiley and Sons, New York, **1993**.
- a) S. Reinhard, P. Soba, F. Rominger, J. Blümel, *Adv. Synth. Catal.* **2003**, 345, 589–602; b) K. D. Behringer, J. Blümel, *Chem. Commun.* **1996**, 653–654; c) S. Reinhard, K. D. Behringer, J. Blümel, *New J. Chem.* **2003**, 27, 776–778.
- a) C. Merckle, J. Blümel, *Adv. Synth. Catal.* **2003**, 345, 584–588; b) C. Merckle, J. Blümel, *Top. Catal.* **2005**, 34, 5–15; c) C. Merckle, S. Haubrich, J. Blümel, *J. Organomet. Chem.* **2001**, 627, 44–54.
- a) Y. Yang, B. Beele, J. Blümel, *J. Am. Chem. Soc.* **2008**, 130, 3771–3773; b) B. Beele, J. Guenther, M. Perera, M. Stach, T. Oeser, J. Blümel, *New J. Chem.* **2010**, 34, 2729–2731.
- N. Lewanzik, T. Oeser, J. Blümel, J. A. Gladysz, *J. Mol. Catal. A: Chemical* **2006**, 254, 20–28.
- a) T. Posset, F. Rominger, J. Blümel, *Chem. Mater.* **2005**, 17, 586–595; b) F. Piestert, R. Fetouaki, M. Bogza, T. Oeser, J. Blümel, *Chem. Commun.* **2005**, 1481–1483.
- M. Bogza, T. Oeser, J. Blümel, *J. Organomet. Chem.* **2005**, 690, 3383–3389.
- R. Fetouaki, A. Seifert, M. Bogza, T. Oeser, J. Blümel, *Inorg. Chim. Acta* **2006**, 359, 4865–4873.
- a) T. M. Duncan, *A Compilation of Chemical Shift Anisotropies*, Farragut Press, Chicago, IL, **1990**; b) C. A. Fyfe, *Solid-State NMR for Chemists*, C. F. C. Press, Guelph, Canada, **1983**; c) M. J. Duer, *Introduction to Solid-State NMR Spectroscopy*, Blackwell Publishing, Oxford, **2004**; d) S. Reinhard, J. Blümel, *Magn. Reson. Chem.* **2003**, 41, 406–416.
- a) S. Brenna, T. Posset, J. Furrer, J. Blümel, *Chem. Eur. J.* **2006**, 12, 2880–2888; b) T. Posset, J. Blümel, *J. Am. Chem. Soc.* **2006**, 128, 8394–8395.
- a) P. W. Clark, J. L. S. Curtis, P. E. Garrou, G. E. Hartwell, *Can. J. Chem.* **1974**, 52, 1714–1720; b) P. W. Clark, G. E. Hartwell, *Inorg. Chem.* **1970**, 9, 1948–1951; c) P. W. Clark, A. J. Jones, *J. Organomet. Chem.* **1976**, 122, C41–C48.
- T. Hirai, L.-B. Han, *Org. Lett.* **2007**, 9, 53–55.
- a) T. Shima, F. Hampel, J. A. Gladysz, *Angew. Chem.* **2004**, 116, 5653–5656; *Angew. Chem. Int. Ed.* **2004**, 43, 5537–5540; b) A. J. Nawara-Hultsch, K. Skopek, T. Shima, M. Barbasiewicz, G. D. Hess, D. Skaper, J. A. Gladysz, *Z. Naturforsch.* **2010**, 65b, 414–424.
- G. Fraenkel, W. R. Winchester, P. G. Williard, *Organometallics* **1989**, 8, 2308–2311.
- J. Cámpora, C. M. Maya, I. Matas, B. Claasen, P. Palma, E. Álvarez, *Inorg. Chim. Acta* **2006**, 359, 3191–3196.
- X-ray data for ligand **17**: $\text{C}_{41}\text{H}_{39}\text{F}_3\text{O}_3\text{P}_4\text{S}$, $M=792.66$, colorless needle, $0.20\times 0.10\times 0.10$ mm³, monoclinic, space group $P2_1/c$ (No. 14), $a=15.693(4)$, $b=12.853(3)$, $c=18.548(4)$ Å, $\beta=94.480(3)^\circ$, $V=3730.0(15)$ Å³, $Z=4$, $\rho_{\text{calc}}=1.412$ g cm⁻³, $F_{000}=1648$, Bruker APEX-II CCD, MoK α radiation, $\lambda=0.71073$ Å, $T=113(2)$ K, $2\theta_{\text{max}}=50.0^\circ$, 29641 reflections collected, 6444 unique ($R_{\text{int}}=0.0708$). Final $GoF=1.000$, $RI=0.0399$, $wR2=0.0808$, R indices based on 4560 reflections with $I>2\sigma(I)$ (refinement on F^2), 469 parameters, 0 restraints. Lp and absorption corrections applied, $\mu=0.313$ mm⁻¹. Further crystallographic data for this structure have been deposited with the Cambridge Crystallographic Data Center as supplementary publication no. CCDC 782510. These data can be obtained free of charge from The Cambridge Crystallographic Data Centre via www.ccdc.cam.ac.uk/data_request/cif.
- M. Baacke, O. Stelzer, V. Wray, *Chem. Ber.* **1980**, 113, 1356–1369.
- G. Tsiavaliaris, S. Haubrich, C. Merckle, J. Blümel, *Synlett* **2001**, 391–393.
- X-ray data for Rh complex **18**: $\text{C}_{49}\text{H}_{49}\text{Cl}_2\text{F}_9\text{O}_3\text{P}_5\text{RhS}$, $M=1217.60$, yellow column, $0.18\times 0.04\times 0.03$ mm³, monoclinic, space group $P2_1/c$ (No. 14), $a=16.005(4)$, $b=19.384(5)$, $c=19.312(5)$ Å, $\beta=113.121(3)^\circ$, $V=5510(3)$ Å³, $Z=4$, $\rho_{\text{calc}}=1.468$ g cm⁻³, $F_{000}=2472$, APEX II, MoK α radiation, $\lambda=0.71073$ Å, $T=296(2)$ K, $2\theta_{\text{max}}=50.0^\circ$, 50109 reflections collected, 9680 unique ($R_{\text{int}}=0.1197$). Final $GoF=1.116$, $RI=0.1096$, $wR2=0.3039$, R indices based on 5747 reflections with $I>2\sigma(I)$ (refinement on F^2), 631 parameters, 131 restraints. Lp and absorption corrections applied, $\mu=0.659$ mm⁻¹. (Note: While the Rh complex could be located with ease, the counteranions and solvent mole-

- cules were found significantly disordered; those containing heavier atoms $[\text{SO}_3\text{CF}_3]^-$, $[\text{PF}_6]^-$, and CH_2Cl_2 could be located and were restrained to keep the bond distances and the thermal ellipsoids meaningful. Residual peaks close to these counter ions and CH_2Cl_2 indicated the possibility of disorder. Given the poor quality of the data, no further attempts were made to model the disorder. Some of the weak residual electron densities could not be deciphered into any realistic solvent. At this stage, the data was squeezed using PLATON which indicated the presence of 141 electrons per unit cell: corresponding well with four pentane molecules [=140 electrons]). Further crystallographic data for this structure have been deposited with the Cambridge Crystallographic Data Center as supplementary publication no. CCDC 782509. These data can be obtained free of charge from The Cambridge Crystallographic Data Centre via www.ccdc.cam.ac.uk/data_request/cif.
- [21] a) S. Herold, A. Mezzetti, L. M. Venanzi, A. Albinati, F. Lianza, T. Gerfin, V. Gramlich, *Inorg. Chim. Acta* **1995**, *235*, 215–231; b) F. Bachechi, J. Ott, L. Venanzi, *Acta Crystallogr.* **1989**, *C45*, 724–728.
- [22] B. E. Hauger, J. C. Huffman, K. G. Caulton, *Organometallics* **1996**, *15*, 1856–1864.
- [23] a) J. Scherer, G. Huttner, O. Walter, B. C. Janssen, L. Zsolnai, *Chem. Ber.* **1996**, *129*, 1603–1615; b) C. Bianchini, C. A. Ghilardi, A. Meli, S. Midollini, A. Orlandini, *Inorg. Chem.* **1985**, *24*, 924–931; c) A. A. Barney, A. F. Heyduk, D. G. Nocera, *Chem. Commun.* **1999**, 2379–2380; d) J. C. Peters, J. D. Feldman, T. D. Tilley, *J. Am. Chem. Soc.* **1999**, *121*, 9871–9872; e) S. Jiménez, J. A. López, M. A. Ciriano, C. Tejel, A. Martínez, R. A. Sánchez-Delgado, *Organometallics* **2009**, *28*, 3193–3202.
- [24] a) C. Merckle, J. Blümel, *Chem. Mater.* **2001**, *13*, 3617–3623; b) J. Blümel, *J. Am. Chem. Soc.* **1995**, *117*, 2112–2113; c) K. D. Behringer, J. Blümel, *J. Liq. Chromatogr.* **1996**, *19*, 2753–2765.
- [25] a) J. Blümel, *Inorg. Chem.* **1994**, *33*, 5050–5056; b) J. Sommer, Y. Yang, D. Rambow, J. Blümel, *Inorg. Chem.* **2004**, *43*, 7561–7563.
- [26] Y. Carpenter, C. A. Dyker, N. Burford, M. D. Lumsden, A. Decken, *J. Am. Chem. Soc.* **2008**, *130*, 15732–15741.
- [27] a) J. Dupont, R. F. deSouza, P. A. Z. Suarez, *Chem. Rev.* **2002**, *102*, 3667–3692; b) P. Wasserscheid, W. Keim, *Angew. Chem.* **2000**, *112*, 3926–3945; *Angew. Chem. Int. Ed.* **2000**, *39*, 3772–3789.
- [28] a) C. Emnet, K. M. Weber, J. A. Vidal, C. S. Consorti, A. M. Stuart, J. A. Gladysz, *Adv. Synth. Catal.* **2006**, *348*, 1625–1634; b) D. Mandal, M. Jurisch, C. S. Consorti, J. A. Gladysz, *Chem. Asian J.* **2008**, *3*, 1772–1782.
- [29] a) H. M. Yeo, B. J. Ryu, K. C. Nam, *Org. Lett.* **2008**, *10*, 2931–2934; b) T. W. Hudnall, Y.-M. Kim, M. W. P. Bebbington, D. Bourissou, F. P. Gabbaï, *J. Am. Chem. Soc.* **2008**, *130*, 10890–10891.
- [30] a) G. C. Welch, D. W. Stephan, *J. Am. Chem. Soc.* **2007**, *129*, 1880–1881; b) G. C. Welch, R. R. San Juan, J. D. Masuda, D. W. Stephan, *Science* **2006**, *314*, 1124–1126.
- [31] a) J. W. Wiench, C. Michon, A. Ellern, P. Hazendonk, A. Iuga, R. J. Angelici, M. Pruski, *J. Am. Chem. Soc.* **2009**, *131*, 11801–11810.
- [32] D. J. Casper, A. V. Sklyarov, S. Hardcastle, T. L. Barr, F. H. Försterling, K. F. Surerus, M. M. Hossain, *Inorg. Chim. Acta* **2006**, *359*, 3129–3138.
- [33] a) *The Handbook of Homogeneous Hydrogenation*, 1st edn., Vols. 1–3 (Eds.: J. G. de Vries, C. J. Elsevier), Wiley-VCH, Weinheim, **2007**; b) M. Wende, R. Meier, J. A. Gladysz, *J. Am. Chem. Soc.* **2001**, *123*, 11490, and references cited therein; c) *Adv. Synth. Catal.* **2003**, *345*, Special Issue on hydrogenation, including, e.g.: W. S. Knowles, *Adv. Synth. Catal.* **2003**, *345*, 3; R. Noyori, *Adv. Synth. Catal.* **2003**, *345*, 15; T. Imamoto, *Adv. Synth. Catal.* **2003**, *345*, 79; d) D. M. Heinekey, A. Lledós, J. M. Lluch, *Chem. Soc. Rev.* **2004**, *33*, 175–182.
- [34] D. Rutherford, J. J. Juliette, Ch. Rocaboy, I. T. Horváth, J. A. Gladysz, *Catal. Today* **1998**, *42*, 381–388.
- [35] a) E. Renaud, M. C. Baird, *J. Chem. Soc. Dalton Trans.* **1992**, *2*, 2905–2906; b) J. M. Buriak, J. C. Klein, D. G. Herrington, J. A. Osborn, *Chem. Eur. J.* **2000**, *6*, 139–150.
- [36] J. P. Collman, K. M. Kosydar, M. Bressan, W. Lamanna, T. Garrett, *J. Am. Chem. Soc.* **1984**, *106*, 2569–2579.
- [37] H. Gao, R. J. Angelici, *Organometallics* **1999**, *18*, 989–995.
- [38] D. R. Anton, R. H. Crabtree, *Organometallics* **1983**, *2*, 855–859.
- [39] a) M. Čapka, J. Hetflejš, V. M. Vdovin, V. E. Fedorov, N. A. Pritula, G. K. Fedorova, *React. Kinet. Catal. Lett.* **1986**, *31*, 41–46; b) J. F. Biellmann, M. J. Jung, *J. Am. Chem. Soc.* **1968**, *90*, 1673–1674.
- [40] K. J. Stanger, Y. Tang, J. Anderegg, R. J. Angelici, *J. Mol. Catal. A* **2003**, *202*, 147–161.
- [41] a) L. Barthe, A. Denicourt-Nowicki, A. Roucoux, K. Philippot, B. Chaudret, M. Hemati, *Catal. Commun.* **2009**, *10*, 1235–1239; b) V. Mévellec, A. Nowicki, A. Roucoux, C. Dujardin, P. Granger, E. Payen, K. Philippot, *New J. Chem.* **2006**, *30*, 1214–1219; c) H. Beyer, K. Chatziapostolou, K. Köhler, *Top. Catal.* **2009**, *52*, 1752–1756; d) A. Roucoux, A. Novicky, K. Philippot, *Nanopart. Catal.* **2008**, *349–388*; e) L. Starkey Ott, R. G. Finke, *Coord. Chem. Rev.* **2007**, *251*, 1075–1100.